JCI The Journal of Clinical Investigation

IL-2-inducible T cell kinase deficiency sustains chimeric antigen receptor T cell therapy against tumor cells

Zheng Fu, … , Qiang Shan, Hongling Peng

J Clin Invest. 2024. https://doi.org/10.1172/JCI178558.

Research In-Press Preview **Hematology** **Immunology**

Despite the revolutionary achievements of chimeric antigen receptor (CAR) T cell therapy in treating cancers, especially leukemia, several key challenges still limit its therapeutic efficacy. Of particular relevance is the relapse of cancer in large part, as a result of exhaustion and short persistence of CAR-T cells in vivo. IL-2-inducible T cell kinase (ITK) is a critical modulator of the strength of T-cell receptor (TCR) signaling, while its role in CAR signaling is unknown. By electroporation of clustered regularly interspaced short palindromic repeats (CRISPR) associated protein 9 (Cas9) ribonucleoprotein (RNP) complex into CAR-T cells, we successfully deleted ITK in CD19-CAR-T cells with high efficiency. Bulk and single-cell RNA sequencing (scRNA-seq) analyses revealed down-regulation of exhaustion and up-regulation of memory gene signatures in ITK-deficient CD19-CAR-T cells. Our results further demonstrated a significant reduction of T cell exhaustion and enhancement of T cell memory, with significant improvement of CAR-T cell expansion and persistence both in vitro and in vivo. Moreover, ITK-deficient CD19-CAR-T cells showed better control of tumor relapse. Our work provides a promising strategy of targeting ITK to develop sustainable CAR-T products for clinical use.

IL-2-inducible T cell kinase deficiency sustains chimeric antigen receptor T cell therapy against tumor cells

Authors

Zheng Fu, [1, 2, 9, 16] Zineng Huang, [1, 3, 4] Hao Xu, [5] Qingbai Liu, [6] Jing Li, [7] Keqing Song, [8] Yating Deng, [1, 3, 4] Yujia Tao, [1, 3, 4] Huifang Zhang, [1, 3, 4] Peilong Wang, [1, 3, 4] Heng Li, [1, 3, 4] Yue Sheng, [1, 3, 4] Aijun Zhou, [6] Lianbin Han, [9] Yan Fu, [9] Chenzhi Wang, [9] Saurav Kumar Choudhary, [10] Kaixiong Ye, [10, 11] Gianluca Veggiani, [12] Zhihong Li, [13, 14] Avery August, [15] Weishan Huang, [12, 15] Qiang Shan, [5] Hongling Peng, [1, 3, 4, 14]

Author affiliation

[1] Department of Hematology, The Second Xiangya Hospital, Central South University, Changsha, Hunan 410011, PR China

[2] Hubei Jiangxia Laboratory, Wuhan, Hubei 430200, PR China

[3] Institute of Hematology, Central South University, Changsha, Hunan 410011, PR China

[4] Hunan Engineering Research Center of Cell Immunotherapy for Hematopoietic Malignancies, Changsha, Hunan 410011, PR China

[5] National Key Laboratory of Immunity and Inflammation, Suzhou Institute of Systems Medicine, Chinese Academy of Medical Sciences & Peking Union Medical College, Suzhou, Jiangsu 215123, PR China

[6] Lianshui People's Hospital of Kangda College Affiliated to Nanjing Medical University, Huai'an, Jiangsu Province, PR China

[7] Key Laboratory of Cluster Science, Ministry of Education of China, School of Chemistry and Chemical Engineering, Beijing Institute of Technology, Beijing, 100081, PR China

[8] Tianjin Mogenetics Biotech Co., Ltd, Tianjin, 300457 PR China

[9] MegaRobo Technologies Co., Ltd, 277 Dongping Road, Suzhou, 215000, PR China

[10] Institute of Bioinformatics, University of Georgia, Athens, GA, 30602, USA

[11] Department of Genetics, Franklin College of Arts and Sciences, University of Georgia, Athens, GA, 30602, USA

[12] Department of Pathobiological Sciences, School of Veterinary Medicine, Louisiana State University, Baton Rouge, LA 70803, USA

[13] Department of Orthopedics, The Second Xiangya Hospital, Central South University, Changsha, PR China

[14] Hunan Key Laboratory of Tumor Models and Individualized Medicine, Changsha, Hunan 410011, PR China

[15] Department of Microbiology and Immunology, College of Veterinary Medicine, Cornell University, Ithaca, NY 14853, USA

[16] Xinyi Biotech Co., Ltd, Lingang, Shanghai, 201306, PR China

Authorship note: ZF, ZH and HX contributed equally to this work. HP, ZF, QS, and WH jointly supervised this work.

Address correspondence to: Hongling Peng, Department of Hematology, The Second Xiangya Hospital, Central South University, Changsha, Hunan 410011, PR China. Phone: +86 0731-85295296; Email: penghongling@csu.edu.cn. Or to: Zheng Fu, Hubei Jiangxia Laboratory, Wuhan, Hubei 430200, PR China. Phone: +86 18120040001; Email: fuzheng_ioz@163.com. Or to: Qiang Shan, National Key Laboratory of Immunity and Inflammation, Suzhou Institute of Systems Medicine, Chinese Academy of Medical Sciences & Peking Union Medical College, Suzhou, Jiangsu 215123, PR China. Phone: +86 0512-62873785; Email: shanq2009@gmail.com. Or to: Weishan Huang, Department of Pathobiological Sciences, School of Veterinary Medicine, Louisiana State University, Baton Rouge, LA 70803, USA. Phone: +01-225-5789467; Email: huang1@lsu.edu.

Conflict of interests

W.H. receives research support from MegaRobo Technologies Corporation and A.A. receives research support from 3M, which were not related to this study. Z.F. and W.H. declare competing financial interests in the form of a pending patent application whose value may be affected by the publication of this manuscript.

Abstract

Despite the revolutionary achievements of chimeric antigen receptor (CAR) T cell therapy in treating cancers, especially leukemia, several key challenges still limit its therapeutic efficacy. Of particular relevance is the relapse of cancer in large part, as a result of exhaustion and short persistence of CAR-T cells in vivo. IL-2-inducible T cell kinase (ITK) is a critical modulator of the strength of T-cell receptor (TCR) signaling, while its role in CAR signaling is unknown. By electroporation of clustered regularly interspaced short palindromic repeats (CRISPR) associated protein 9 (Cas9) ribonucleoprotein (RNP) complex into CAR-T cells, we successfully deleted *ITK* in CD19-CAR-T cells with high efficiency. Bulk and single-cell RNA sequencing (scRNA-seq) analyses revealed down-regulation of exhaustion and up-regulation of memory gene signatures in ITK-deficient CD19-CAR-T cells. Our results further demonstrated a significant reduction of T cell exhaustion and enhancement of T cell memory, with significant improvement of CAR-T cell expansion and persistence both in vitro and in vivo. Moreover, ITK-deficient CD19-CAR-T cells showed better control of tumor relapse. Our work provides a promising strategy of targeting ITK to develop sustainable CAR-T products for clinical use.

Introduction

Chimeric antigen receptor (CAR) T cell therapy, as an innovative cellular immunotherapy, has been used in leukemia (1), solid tumors (2), and several other diseases such as autoimmunity (3, 4) and cardiac injury (5). Currently, a total of nine CAR-T products have been approved for clinical therapy. Despite the remarkable clinical efficacy of CAR-T therapy in leukemia, especially in B cell malignancy (1), there are still many challenges limiting its therapeutic efficacy. Relapse of tumor remains the major obstacle to be addressed, especially in CD19-targeted CAR-T therapy which even about 40%–60% of patients achieving a complete response (CR) eventually experience relapse (1, 6, 7). For example, a recent study reported that CAR-T treatment for diffuse

large B-cell lymphoma (DLBCL) showed about 43% progression 8 months after CAR-T infusion (8). The efficacy of CAR-T cell therapy remains largely to be improved in cancer treatment.

Severe T cell exhaustion in the tumor environment and the relatively short persistence of CAR-T cells in vivo are among the key obstacles affecting the efficacy of CAR-T therapy (1, 6, 7, 9). Recently, there have been many efforts towards decreasing exhaustion and promoting the persistence of CAR-T cells. Combinations of CAR-T therapy with PD-1 blockade or knockout have been investigated in several tumors and showed promising outcomes (10, 11). However, the application of these strategies was restricted due to the limited PD-1 expression in certain tumors and the systemic side effects of PD-1 blockade. In addition, targeted deletion or inhibition of genes, such as *TGFBRII*, *NR4A*, *DNMT3A*, BET proteins, Ragnase-1 and Roquin-1, have been shown to reduce T cell exhaustion, promote CAR-T cells persistence and/or enhance antitumor activity (12-16). It has been reported that SRC family kinase (SFK) LCK, a critical kinase for T-cell receptor (TCR) signaling, promotes strong signaling that tends to lead to exhaustion in CAR-T cells (17). LCK-deficient CAR-T cells show enhanced therapeutic efficacy with reduced exhaustion and enhanced memory in vivo (17). Additionally, previous studies have shown that transient treatment with dasatinib, a multi-targeted tyrosine kinase inhibitor that targets ABL, SRC and c-KIT, reduces the expression of exhaustion markers and increases the expression of memory-associated markers through epigenetic remodeling (18-20). However, current knowledge and approaches are still quite limited in addressing these obstacles.

The Tec family non-receptor tyrosine kinase IL-2-inducible T cell kinase (ITK), predominantly expressed in T cells, is a crucial signaling mediator downstream of TCR and regulates the strength of TCR signaling (21). ITK plays critical roles in T cell activation and differentiation (22). In *Itk* knockout (hereafter as *Itk*$^{-/-}$) mice, T cells spontaneously develop a memory-like phenotype independent of specific antigenic stimulation (23, 24), and can rapidly produce IFN-γ upon stimulation (23, 25). In mouse models of antigen-specific CD8^{+} T cell development following infections, naïve *Itk*$^{-/-}$ CD8^{+} T cells also showed significantly enhanced memory development (26,

27). Similarly, naive *Itk*$^{-/-}$ T cells expanded significantly better than WT cells under lymphogenic conditions (28). In the clinic, ibrutinib, a Bruton's Tyrosine Kinase (BTK) inhibitor for B cell leukemia treatment, has been used in combination with CD19-CAR-T cells for chronic lymphocytic leukemia (CLL) therapy (29). An increased response rate of CAR-T cell therapy in CLL patients with these combination therapy has been reported (30). Due to the C-terminal kinase domain has high levels of structural similarity between ITK and other Tec family members, BTK inhibitors like ibrutinib exhibit off-target effects on ITK. It has been reported that Ibrutinib could directly reduce CD8^{+}T cell exhaustion independent of BTK (31). Furthermore, chronic TCR activation drives T cell exhaustion and tempering TCR signaling by ITK inhibition or deletion will reduce T cell exhaustion in mice (32-34). However, the intrinsic role of ITK in CAR-T cells against tumors remains unaddressed.

Here, by combining the clustered regularly interspaced short palindromic repeats (CRISPR) associated protein 9 (Cas9) gene editing technology with multiple in vitro and in vivo models of CD19-CAR-T cell therapy, we showed that ITK deficiency in CD19-CAR-T cells significantly improved expansion, reduced cell exhaustion and enhanced memory of CAR-T cells. ITK-deficient CD19-CAR-T cells showed better control of tumor relapse, leading to more sustainable therapeutic effects. In addition, ITK deficiency in CAR-T cells derived from CLL patients attenuated T cell exhaustion, a critical issue in CLL patients (35), thereby potentially addressing a challenge in CAR-T cell therapy for CLL patients. Our results suggest that deletion of *ITK* during CAR-T cell production may be a useful strategy for the development of sustainable and functional CAR-T cell therapy, which will potentially benefit patients whose T cell functional quality are low, as well as those who suffer from tumor relapses.

Results

ITK deficiency attenuates immediate cytotoxicity of CD19-CAR-T cells

CAR-T cells targeting human CD19 (hereafter referred to as CD19-CAR-T cells) were obtained

via lentiviral transduction of a third generation CAR (Figure 1A), and *ITK* deletion in CD19-CAR-T cells was performed through electroporation of Cas9-single guide RNA (sgRNA) ribonucleoprotein (RNP) complex (Figure 1B). Notably, we observed a modest impact on the expression of several functional molecules in T cells following lentiviral transduction and electroporation (Supplemental Figure 1, A-D). However, there was no significant impact on the non-specific killing activity of T cells against MEC1 cells (a CD19-expressing CLL tumor cell line) or on T cell expansion following these procedures (Supplemental Figure 1, E-G). The gene editing efficiency of *ITK* was 86.6% for sgRNA1 and 96.9% for sgRNA2 (Figure 1C and Supplemental Figure 1, H and I), with sgRNA1 displaying less off-target effects than sgRNA2 (Supplemental Figure 1, J and K). Thus, sgRNA1 was used in the following experiments in this study unless otherwise noted. Efficient deletion of ITK (ITK-KO) was further confirmed at the protein level by western blotting (Figure 1D). Reduced activation of TCR downstream signaling molecules, including phosphorylated PLCγ1 (p-PLCγ1), phosphorylated ERK1/2 (p-ERK1/2), and phosphorylated p70S6 (p-p70 S6), were observed in ITK-KO CD19-CAR-T cells after co-cultured with MEC1 cells (Supplemental Figure 1L). This indicates that ITK deficiency impairs TCR downstream signaling in ITK-KO CD19-CAR-T cells. Continued monitoring of CAR-T cells co-cultured with MEC1 cells suggested that both ITK-KO CD19-CAR-T cells and control CD19-CAR-T cells were able to efficiently kill MEC1 cells (Supplemental Video 1-3). The cytotoxic activity of ITK-KO CD19-CAR-T cells was further assessed in vitro against a panel of cell line models of B cell malignancy (including two CLL cell lines expressing CD19 (MEC1 and HG3) and Raji cell line derived from Burkitt lymphoma). The tumor killing ability of ITK-KO CD19-CAR-T cells was compared to control CD19-CAR-T cells that were electroporated with a RNP complex containing a non-targeting sgRNA (nt-KO). Deletion of *ITK* slightly reduced the cytotoxic function of CD19-CAR-T cells compared to nt-KO CD19-CAR-T cells in all tested cell lines (Figure 1, E-G). However, ITK-KO CD19-CAR-T cells showed no obvious changes in IFN-γ, TNF-α, and Granzyme B expression by flow cytometric analyses, as compared to nt-KO CD19-CAR-T cells (Figure 1, H

and I, and Supplemental Figure 1, M and N). Furthermore, IL-17A, FOXP3 and Th2-associated cytokines were expressed at low levels, with minimal differences observed between nt-KO and ITK-KO CD19-CAR-T cells (Supplemental Figure 1O). These results suggest that ITK deficiency in CD19-CAR-T cells attenuated the immediate cytotoxic effects against tumor cells but did not profoundly affect the production of effector cytokines.

ITK deficiency promotes long-term expansion of CD19-CAR-T cell in vitro

To further determine the role of ITK in CD19-CAR-T cells, we examined the cell expansion, proliferation and apoptosis in ITK-KO CD19-CAR-T cells and nt-KO CD19-CAR-T cells after co-culture with tumor cells. ITK-KO CD19-CAR-T cells exhibited similar rates of cell expansion at the early time points (e.g., before day 20 after co-culture) compared to nt-KO CD19-CAR-T cells (Figure 2, A-C). However, we observed significant improvements in the expansion of ITK-KO CD19-CAR-T cells at later time points compared to nt-KO CD19-CAR-T cells, (both $CD4^+$ and $CD8^+$ CD19-CAR-T cells) (Figure 2, A-C, and Supplemental Figure 2). Annexin V staining revealed that the apoptosis of nt-KO CAR-T cells significantly increased 45 days after in vitro culture. In contrast, ITK-KO CD19-CAR-T cells displayed a significantly lower level of apoptosis at this time point (Figure 2, D and E). Furthermore, Ki-67 staining demonstrated that the proliferation of both nt-KO and ITK-KO CD19-CAR-T cells decreased over time, but this reduction was smaller in ITK-KO CD19-CAR-T cells compared to nt-KO CAR-T cells at day 30 (Figure 2, F and G). Overall, these data indicate that ITK deficiency enhances the long-term expansion with significantly better survival and slower reduction of proliferation of CD19-CAR-T cells in vitro.

Transcriptomic regulation by ITK in CD19-CAR-T cells

To investigate how ITK regulates the transcriptome of CAR-T cells, we first conducted high-throughput RNA sequencing (bulk RNA-seq) on ITK-KO and nt-KO CD19-CAR-T cells. A total of 1319 genes were significantly differentially expressed between nt-KO and ITK-KO CD19-CAR-T

cells (fold change ≥ 1.5, P ≤ 0.05) (Figure 3A and Supplemental Figure 3, A and B). Among these, 797 were increased, while 522 were decreased in the ITK-KO CD19-CAR-T cells (Figure 3A and Supplemental Figure 3B). In line with the critical role of ITK in TCR signaling, we observed a significant enrichment of differentially expressed genes involved in several immune signaling pathways downstream of the TCR signaling, such as cytokine-cytokine receptor interaction and cytokine-mediated signaling pathways (Figure 3B and Supplemental Figure 3C) by Kyoto Encyclopedia of Genes and Genomes (KEGG) and Gene Ontology (GO) analyses. In addition, multiple genes involved in T cell activation, such as *TNFSF4*, *TNFSF14*, *XCL1*, *XCL2* and *TBX21*, were significantly decreased in the ITK-KO CD19-CAR-T cells (Figure 3C). Furthermore, transcription of several key JAK-STAT signaling genes, such as *STAT1*, *STAT2*, *STAT3* and *STAT4*, but not *STAT6*, were significantly increased in ITK-KO CD19-CAR-T cells (Figure 3C). Enhancement of STAT1, STAT3 and STAT5, but not STAT6, had been shown to promote stem cell memory and effector CAR-T cells (36). Our observations suggested that ITK deficiency regulated TCR signaling in CD19-CAR-T cells and may promote effector/memory formation in CAR-T cells. Indeed, several genes associated with naïve or progenitor-memory T cells, including *SELL* (encoding CD62L), *IL7R* (encoding CD127), *TCF7* (encoding TCF1), *KLF2* and *LEF1*, were significantly increased in the ITK-KO CD19-CAR-T cells (Figure 3, C and D). Gene set enrichment analysis (GSEA) further indicated significant enrichment of genes associated with T cell effector/memory phenotype in the ITK-KO CD19-CAR-T cells (Figure 3E). In contrast, genes involved in T cell exhaustion(37), such as *PDCD1* (encoding PD-1) and *LAG3*, were significantly decreased in ITK-KO CD19-CAR-T cells (Figure 3C). Together, our results suggested that ITK may affect CAR-T cell activation, decrease T cell exhaustion, and promote memory formation.

To gain further insights into how ITK regulates the heterogeneity and transcriptomic profile of CAR-T cells, we conducted single-cell RNA sequencing (scRNA-seq) on ITK-KO and nt-KO CD19-CAR-T cells, following stimulation by MEC1 cells for 48 hours. By merging both nt-KO and ITK-KO CD19-CAR-T cells, 8 T cell populations with different states were identified (Figure 3, F

and G and Supplemental Figure 3, D-F). Interestingly, while other populations were at similar level between nt-KO and ITK-KO CD19-CAR-T cells, we observed that the memory-progenitor population in ITK-KO CD19-CAR-T cells was almost two-fold higher compared to in nt-KO CD19-CAR-T cells (33.74% in ITK-KO CD19-CAR-T cells *vs* 13.94% in nt-KO CD19-CAR-T cells) (Figure 3, F and G and Supplemental Figure 3, D-F). In line with the observations from bulk RNA-seq, lower expression of *LAG3* was observed in ITK-KO CD19-CAR-T cells (Figure 3H). In contrast, multiple genes highly expressed in memory T cells, such as *TCF7* (encoding TCF1), *KLF2* and *IL7R* (encoding CD127), showed increased expression in ITK-KO CD19-CAR-T cells, especially within the memory-progenitor T cell population (Figure 3, I-K). This is consistent with the observed increase of *TCF7*, *KLF2* and *IL7R* expression in ITK-KO CD19-CAR-T cells in the bulk RNA-seq analysis (Figure 3, C and D and Supplemental Figure 3G). These findings collectively indicate that ITK deficiency may reduce exhaustion and enhance T cell memory fate in CD19-CAR-T cells.

ITK deficiency reduces exhaustion and promotes memory phenotype in CD19-CAR-T cells in vitro

To further investigate the role of ITK in regulating T cell activation, exhaustion, and memory, we determined the protein expression of multiple key molecules involved in these processes between nt-KO and ITK-KO CD19-CAR-T cells under steady state or co-cultured with tumor cells. Despite a slight decrease in CD69 expression in ITK-KO CD19-CAR-T cells under steady-state conditions (Figure 4, A and B), we observed a significant up-regulation of CD69 expression in the ITK-KO CD19-CAR-T cells upon stimulation with MEC1 cells, reaching levels comparable to those observed in nt-KO CD19-CAR-T cells (Figure 4, A and B). These results indicated that ITK deficiency did not affect the activation of CD19-CAR-T cells following stimulation by the targeted tumor cells. Interestingly, we noted a significant down-regulation of the expression of multiple co-inhibitory molecules associated with CAR-T cell exhaustion (37), including LAG-3, PD-1, and TIM-

3, in ITK-KO CD19-CAR-T cells compared to nt-KO CD19-CAR-T cells 48 hours after co-culture with tumor cells (Supplemental Figure 4, A-D). This down-regulation was observable in ITK-KO CD19-CAR-T cells both at the steady state and after co-culture with MEC1 cells or Raji cells (Supplemental Figure 4, A-F). Moreover, down-regulation of co-inhibitory molecules, including PD-1, TIGIT, TIM-3 and CTLA4, was observed in ITK-KO CD19-CAR-T cells 15 days after co-culture with MEC1 cells (Figure 4, C and D, and Supplemental Figure 4, G and H). Remarkably, the decreased expression of PD-1, LAG-3, and TIM-3 in ITK-KO CD19-CAR-T cells, compared to nt-KO CD19-CAR-T cells, remained significant after multiple rounds of exposure to the targeted tumor cells (Figure 4E). We also analyzed the cytotoxic potential of ITK-KO CD19-CAR-T cells following repeated exposure to cancer cells. While we observed a limited but significant decrease in their cytotoxic effect in the initial phases of antigen exposure (e.g., rounds 1 through 6, and round 8), the tumor-killing ability of ITK-KO CD19-CAR-T cells reached comparable levels to nt-KO CD19-CAR-T cells at later time-points (e.g., rounds 7 and 9) (Figure 4F and Supplemental Figure 4I). These data suggest that ITK-KO CD19-CAR-T cells retain good anti-tumor activity following repeated exposure to $CD19^{+}$ cancer cells, probably due to less T cell exhaustion and enhanced memory development. In fact, following exposure to tumor cells, there was a significantly decreased fraction of terminally differentiated cells and an increased fraction of central memory cells in ITK-KO CD19-CAR-T cells compared to nt-KO CD19-CAR-T cells (Figure 4, G and H, and Supplemental Figure 4J and K). Together, these results suggest that ITK deficiency decreases T cell exhaustion and enhances memory fate of CD19-CAR-T cells in vitro.

ITK deficiency enhances expansion and long-term persistence of CD19-CAR-T cells in vivo

To test the long-term effects of *ITK* deletion on CD19-CAR-T cells in vivo, we first used a CLL mouse model of NOD-*Prkdc*^{scid}*Il2rγ*^{null} (NPG) mice bearing MEC1 tumor cells (injected intraperitoneally) followed by infusion with ITK-KO or nt-KO CD19-CAR-T cells (Figure 5A). In this tumor model, both ITK-KO and nt-KO CD19-CAR-T cells efficiently cleared tumor cells 14 days

after infusion (Supplemental Figure 5A). There was no significant difference in the body weight of mice between ITK-KO and nt-KO CD19-CAR-T cell-injected groups (Supplemental Figure 5B). Interestingly, upon tumor clearance, the abundance of ITK-KO CD19-CAR-T cells peaked at a significantly higher level than nt-KO CD19-CAR-T cells (Figure 5, B and C), in agreement with the enhanced expansion of ITK-KO CD19-CAR-T cells. In addition, while nt-KO CD19-CAR-T cells rapidly contracted to levels that were nearly undetectable, ITK-KO CD19-CAR-T cells remained in circulation at a significantly higher level even 77 days post-infusion (Figure 5, B and C). Moreover, ITK-KO CD19-CAR-T cells showed significantly lower expression of multiple co-inhibitory molecules that are associated with T cell exhaustion, including LAG-3, PD-1, TIM-3, TIGIT and CTLA4 (Figure 5, D and E). As expected, significant decrease of apoptosis (indicated by Annexin V) and significant increase of proliferation (indicated by Ki-67) were observed in ITK-KO CD19-CAR-T cells compared to nt-KO CD19-CAR-T cells (Figure 5, F and G, and Supplemental Figure 5, C and D). Notably, we observed a high level of apoptosis in CAR-T cells (Supplemental Figure 5D), which may be because that these apoptotic CAR-T cells were in the contraction phase at this time point and were not rapidly cleared in the immune-deficient recipients. Remarkably, there were more effector memory and less terminally differentiated CAR-T cells in mice injected with ITK-KO CD19-CAR-T cells compared to controls (Figure 5H, and Supplemental Figure 5E). As enhanced memory cell phenotype has been correlated with improved long-term CAR-T cell therapeutic effects (36, 38, 39), our results suggest that ITK deficiency enhances expansion and long-term persistence of CD19-CAR-T cells due to ITK-mediated reduction of exhaustion and improvement of memory in CAR-T cells in vivo.

The CLL cell line MEC1 could also be subcutaneously injected into NPG mice and form a solid tumor (40). We further tested the impact of *ITK* deletion on CD19-CAR-T cells in this mouse model of CLL with solid tumor (41) (Figure 5I). Consistent with the previous intraperitoneal MEC1 injection model, ITK-deficient CD19-CAR-T cells not only expanded to a higher peak level but

also persisted much longer in the peripheral blood after injection into the MEC1-bearing NPG mice (Figure 5, J and K). Interestingly, we found that ITK-deficient CD19-CAR-T cells showed a slight delay in the pattern of increase compared to nt-KO CD19-CAR-T cells (Figure 5, J and K). This observation might be consistent with the results that mice from nt-KO CD19-CAR-T cell injected groups showed a trend of faster tumor cell clearance, although with no significant difference compared to mice from ITK-KO CD19-CAR-T cells injected groups (Supplemental Figure 5F). The body weight of mice between ITK-KO and nt-KO CD19-CAR-T cell injected groups also showed no significant difference in this tumor model (Supplemental Figure 5G). Overall, above results show that ITK deficiency enables enhanced expansion and long-term persistence of CD19-CAR-T cells in vivo in pre-clinical animal models of CLL.

ITK-deficient CAR-T cells significantly improve control of tumor relapse in vivo

As we observed significantly improved expansion and long-term persistence of ITK-deficient CD19-CAR-T cells compared to nt-KO CD19-CAR-T cells in vivo, we speculated that mice receiving ITK-KO CD19-CAR-T cells might be better protected against tumor relapse. The Raji cell xenograft mouse model is known to relapse after the first wave of tumor clearance by CAR-T cells (42, 43). Therefore, we used this model (Figure 6A) to assess the function of ITK in CD19-CAR-T cell activity against tumor relapse. In this model, ITK-KO CD19-CAR-T cells showed significantly enhanced expansion and long-term survival compared to nt-KO CD19-CAR-T cells (Figure 6, B and C), as ITK-KO CD19-CAR-T cells displayed lower levels of apoptotic cells and increased proliferation (Figure 6, D and E, and Supplemental Figure 6, A and B). In addition, ITK-KO CD19-CAR-T cells showed significantly reduced levels of the T cell exhaustion molecules, LAG-3 and TIGIT (Figure 6, F and G, and Supplemental Figure 6, C and D). Raji cell-bearing mice that were treated without CAR-T cells showed progression of tumor growth and succumbed to tumor growth before 40 days after Raji cell injection (Figure 6, H and I). In contrast, tumor-grafted mice that received nt-KO CD19-CAR-T cells cleared tumors within 21 days but showed notable

cancer relapse approximately 56 days after CAR-T cell injection (Figure 6, H and I). This group of mice also finally died of uncontrolled tumor relapse (Figure 6, H and I). Interestingly, even after tumor relapse at day 56, animals that received ITK-KO CD19-CAR-T cells exhibited better control of the relapsed tumor, leading to significantly improved survival (Figure 6, H and I, and Supplemental Figure 6E). No significant difference in body weight was observed between groups of mice that received either nt-KO or ITK-KO CD19-CAR-T cells (Supplemental Figure 6F). Above results demonstrate that ITK deficiency in CD19-CAR-T cells promotes CAR-T cell expansion and survival in vivo and enables better control of tumor relapse.

Higher frequency of effector memory and central memory CAR-T cell populations were observed in mice that received ITK-KO CD19-CAR-T, compared to mice that received nt-KO CD19-CAR-T cells (Figure 6J and Supplemental Figure 6G). To further validate the long-term effector-memory function of ITK-KO CD19-CAR-T cells in vivo, we tested the memory-recall responses of ex-vivo ITK-KO CD19-CAR-T cells, from Raji-grafted mice at day 50 after CAR-T cell injection (when the first wave of Raji growth had been controlled). As shown, ex-vivo ITK-KO CD19-CAR-T cells showed significant control of Raji cell growth and expansion when co-cultured with Raji cells (Figure 6, K-M). Furthermore, we observed an increase of IFN-γ, TNF-α and Granzyme B expression in ex-vivo ITK-KO CD19-CAR-T cells after co-culture with Raji cells (Figure 6N and Supplemental Figure 6H). Together, our results suggest that ITK deficiency in CD19-CAR-T cells promotes CD19-CAR-T cell memory fate associated with less T cell exhaustion and better in vivo persistence, providing a potentially more sustainable CAR-T cell therapy.

ITK deficiency attenuates exhaustion and promote memory phenotype in CD19-CAR-T cells derived from CLL patients

T cells from CLL patients show notable exhaustion (35), and prior treatment with ibrutinib, a BTK inhibitor, was associated with an increased response rate of CAR-T cell therapy in CLL patients (30). Since ibrutinib can also inhibit ITK (44), we speculate that the improved CAR-T therapeutic

effects in ibrutinib-treated CLL patients are in part due to the inhibition of ITK in CAR-T cells. Therefore, we derived CD19-CAR-T cells from PBMCs of CLL patients (referred to as CLL-CAR-T cells) and investigated the role of ITK in CLL-CAR-T cells. Notably, while the total cell number of PBMCs from CLL patients was comparable to that from healthy donors (Supplemental Figure 7A), the proportion of T cells was significantly reduced in PBMCs from CLL patients (Supplemental Figure 7, B-E). The viability of T cells from CLL patients was similar to that of T cells from healthy donors (Supplemental Figure 7F). ITK-KO CLL-CAR-T cells showed slightly increased TNF-α expression, following stimulation (Figure 7, A and B). In addition, a slight decrease in T cell activation as indicated by CD69 was observed in ITK-KO CLL-CAR-T cells when co-cultured with MEC1 cells (Figure 7, C and D). And as expected, ITK-KO CLL-CAR-T cells showed a significant decrease in the expression of co-inhibitory molecules, including LAG-3, PD-1 and TIM-3 (Figure 7, E and F). Furthermore, ITK-KO CLL-CAR-T cells exhibited significantly lower apoptosis when co-cultured with MEC1 cells for 15 days compared to nt-KO CLL-CAR-T cells (Figure 7, G and H). ITK-KO CLL-CAR-T cells also demonstrated enhanced expansion in vitro compared to nt-KO CLL-CAR-T cells, particularly at later time points (Supplemental Figure 7G), despite having attenuated cytotoxic function, especially at low E:T ratio (Supplemental figure 7H).

To further determine whether inhibiting ITK kinase activity during the production of CAR-T cells could mimic *ITK* deletion, we investigated the effects of PF-06465469 (a potent ITK inhibitor that also inhibits BTK) and ibrutinib on CLL-CAR-T cells. Both PF-06465469 and ibrutinib significantly decreased PD-1 and LAG-3 expression (Figure 7, I and J, and Supplemental Figure 7, I-N), suggesting a potential decrease of exhaustion in CLL-CAR-T cells. Notably, CD69 expression was also significantly decreased after PF-06465469 and ibrutinib treatment (Figure 7, I and J, and Supplemental Figure 7, M and N), indicating reduced T cell activation. Consistent with the expectation from previous results, there was a significantly increased in the fraction of central memory cells in CLL-CAR-T cells 15 days after PF-06465469 treatment (Figure 7, K and L),

suggesting that ITK inhibition could also promote T cell memory in CD19-CAR-T cells generated from CLL patient.

Of note, infusion of the inhibitor-treated CLL-CAR-T cells or control DMSO-treated CLL-CAR-T cells into MEC1-bearing mice revealed only a trend but no significant increase of CLL-CAR-T cells (Supplemental Figure 7, O-R). This data suggests that while inhibiting ITK during CAR-T cell production can temporarily alleviate exhaustion and promote memory phenotype in CLL-CAR-T cells in vitro, genetically targeting or continuously pharmacological inhibition of the T cell-intrinsic ITK signaling is probably required for sustaining the long-term responses of CAR-T cells against tumors.

To assess the long-term in vivo effects of *ITK* deletion on CLL-CAR-T cells, we employed a CLL mouse model using NPG mice injected intravenously with MEC1 tumor cells, followed by infusion with ITK-KO or nt-KO CLL-CAR-T cells (Figure 8A). The results showed that ITK-KO CLL-CAR-T cells exhibited better expansion and long-term persistence compared to nt-KO CLL-CAR-T cells (Figure 8, B and C). Additionally, ITK-KO CLL-CAR-T cells showed increased proliferation and reduced apoptosis compared to nt-KO CLL-CAR-T cells (Supplemental Figure 8, A-D). There was reduced exhaustion and enhanced memory phenotype in ITK-KO-CLL-CAR-T cells compared to nt-KO CLL-CAR-T cells (Figure 8, D-G, and Supplemental Figure 8E). Furthermore, ITK-KO CLL-CAR-T cells showed better control of tumor relapse (Figure 8, H and I, and Supplemental Figure 8F). Notably, mouse body weights were similar between the groups treated with ITK-KO and nt-KO CLL-CAR-T cells (Supplemental Figure 8G). Above results suggest that CLL-CAR-T cells with ITK deficiency exhibit enhanced efficacy in controlling tumor relapse.

Altogether, our results suggest that ITK deficiency could reduce exhaustion and promote memory in CD19-CAR-T cells, improving the expansion and long-term persistence of CAR-T cells in vivo. This contributes to better control of tumor relapse and potentially improves clinical outcomes.

Discussion

CAR-T therapy has emerged as a groundbreaking treatment for various hematologic malignancies. However, the efficacy and long-term sustainability of CAR-T cells remain challenging due to issues such as T cell exhaustion, relatively short persistence in vivo and antigenic escape (45, 46). Furthermore, CAR-T cell therapy faces a substantial hurdle given its autologous nature, which necessitates using a patient's own T cells for CAR-T cell production. Obtaining a sufficient quantity and quality of T cells proves exceedingly difficult, primarily due to the occurrence of T cell lymphopenia and exhaustion prevalent in cancer patients, including those with chronic lymphocytic leukemia (CLL) (47). These limitations cause concerns about the safety, efficacy, and accessibility of CAR-T cell therapy. Our data provide direct evidence for the cell intrinsic role of ITK in regulation of expansion and memory development, as well as exhaustion in CAR-T cells. Deletion of *ITK* during CAR-T cell production leads to enhanced CAR-T cell expansion and memory development, along with reduced cell apoptosis and exhaustion upon repeated exposures to tumor cells. This improved CAR-T cell sustainability is of particular interest for controlling tumor relapse.

One of the interesting findings of this study is the attenuation of immediate cytotoxicity in ITK-deficient CAR-T cells against tumor cells. While these cells exhibit slightly reduced cytotoxicity against tumor cells, they do not show a significant decline in the production of critical effector cytokines such as IFN-γ, TNF-α, and Granzyme B. This suggests that ITK deficiency primarily affects the immediate cytotoxic effects of CAR-T cells, which may not be as critical for long-term anti-tumor responses. Indeed, previous studies demonstrated that ITK is not required for T cell activation, but it rather promotes the strength of TCR signaling and thus TCR-dependent cytotoxic T cell function (48). This ITK-mediated strong TCR signaling can tune down T cell responses to cytokines that can drive T cell expansion, survival and memory development, such IL-2 and IL-4 (49).

Our study reveals that ITK-deficient CAR-T cells exhibit enhanced expansion and long-term survival in response to tumor antigen stimulation. This is crucial for maintaining therapeutic

efficacy over extended periods. While initial expansion rates are similar between ITK-deficient and control CAR-T cells, the former outperform at later stages. This could be attributed to reduced apoptosis and prolonged proliferation in ITK-deficient CAR-T cells. Regarding the in vitro expansion of CAR-T cells, it appears that $CD4^+$T cells exhibit greater improvement for expansion compared to $CD8^+$T cells following *ITK* knockout. This difference might be due to the varying expression levels of IL-2 receptors on $CD4^+$ T cells and $CD8^+$ T cells (50). During the in vitro expansion of CAR-T cells, relatively high level of IL-2 was added to the culture medium to produce sufficient CAR-T cells for clinical use (51-54). Given the higher expression of IL-2 receptors in $CD8^+$T cells (50), the extend of IL-2 downstream signaling activation might be closer to saturation in $CD8^+$T cells than in $CD4^+$T cells.

In addition, our current knowledge of the role of ITK in T cell exhaustion is very limited. Importantly, this study shows that ITK deficiency leads to reduced T cell exhaustion, as evidenced by lower expression of exhaustion markers such as LAG-3, PD-1, TIM-3, TIGIT, and CTLA4. Moreover, the transcriptomic and single-cell RNA sequencing analyses indicate that ITK-KO CAR-T cells are characterized by a more marked central memory phenotype, which could contribute to their sustained anti-tumor activity. Recently it has been demonstrated that tumor-infiltrating $TCF1^+$ T cells have long-term memory, and are capable of self-renewal and persistent control of tumor growth. It is possible that the up-regulation of TCF1, a dominant transcription factor negatively regulating T cell terminal differentiation and exhaustion, observed in ITK-KO CAR-T cells might prevent the progressive exhaustion and maintain a long-term memory.

We showed that while pharmacological ITK inhibition could mitigate T cell exhaustion and promote memory phenotype in CAR-T cells derived from patients with CLL, it only showed a trend but no significant increase of CLL-CD19-CAR-T cells in the tumor-bearing mouse model in vivo. These observations may suggest that transient inhibition of ITK may not be enough to maintain CAR-T cell status with low exhaustion and better memory. Genetic deletion or silencing of *ITK* at least for a certain is probably required for efficiently and persistently reduce T cell exhaustion and

promote T cell memory in CAR-T cells. Of note, the control of relapse varied among individual tumor-bearing mice, which might be attributed to biological variation in the recipient mice. This variability suggests that clinical outcomes might differ among patients when using ITK-deficient CAR-T cells for managing tumor relapse. Exploring host factors that might influence the effectiveness of ITK-deficient CAR-T cells in controlling tumor relapse would be a valuable direction for future research.

Previous studies have shown that transient treatment with dasatinib reduces expression of exhaustion markers and increases expression of stem cell memory-associated markers, and improves tumor clearance (18, 19). Investigate whether long-term dasatinib treatment or permanent deletion of dasatinib targets could enhance CAR-T cell persistence and better control tumor relapse in vivo would be an intriguing area for future research.

Since lentivirus transduction and electroporation, which might act as stimulatory factors affecting T cell activation and function, are commonly used in CAR-T cell production and gene editing, examining their overall impact on CAR-T cells in further studies would be beneficial. Additionally, although we selected an ITK-targeting sgRNA with less overall off-target effects and with the top predicted off-target sites outside the coding sequences of known genes, potential off-target effects in introns or intergenic regions still should be considered, as these regions may affect gene expression (55).

It has been reported that ITK deficiency may impact Th17 development and promote Treg generation (56-60). Additionally, several studies have shown that *Itk*$^{-/-}$ CD4 T cells exhibit defects in producing Th2 cytokines in mice (61, 62). Our findings indicate that the expression of IL-17A, IL-4, IL-13 and FOXP3 were low in the CAR-T cells, with minimal differences observed between ITK-KO and nt-KO CAR-T cells. The low expression of these cytokines may be attributed to the in vitro culture environment, where CAR-T cells are exposed to tumor cells, potentially favoring Th1 cytokine expression. However, the effects of ITK on the expression of these molecules still should be further considered in clinical applications involving human CAR-T cells, which may

encounter more complex environmental conditions. The expectation of inhibiting Th2, Th17 and favoring Treg generation effects by ITK deficiency in CAR-T cells may potentially result in attenuated cytokine release syndrome (CRS) and immune effector cell-associated neurotoxicity syndrome (ICANS) in clinical settings. Moreover, the absence of ITK has been shown to attenuate T cell migration to several peripheral organs, such as the intestine and brain (63-66), which may further contribute to reduced CRS and ICANS during ITK-KO CD19-CAR-T cell therapy. Investigating these aspects in future studies could provide valuable insights.

In conclusion, this study demonstrates that ITK deficiency enhances the expansion, with reduction of exhaustion, and improvement of the long-term therapeutic effects of CAR-T cells. These findings offer promising insights into the development of more effective and sustainable CAR-T cell therapies for a broad spectrum of cancers. Further research and clinical trials are warranted to validate the clinical applicability of targeting ITK in CAR-T cell therapy.

Methods

Sex as a biological variable.

Our study examined male and female animals, and similar findings are reported for both sexes.

Mice

NOD.Cg-Prkdc^{scid} Il2rg^{tm1Vst}/Vst (NPG) mice were from Beijing Vitalstar Biotechnology ranging from 6 to 8 weeks of age. Experiments were performed with both male and female mice unless otherwise indicated. For MEC1 cell-derived xenograft models, NPG mice were implanted with 1.0×10^7 MEC1 cells expressing firefly luciferase intraperitoneally in the left flank, or with 1.0×10^7 MEC1 cells subcutaneously, or with 5.0×10^6 MEC1 cells expressing firefly luciferase via the lateral tail veins, using a 27-gauge needle. Five to ten days post-engraftment, mice bearing tumor were intravenously administered 2.0×10^6 nt-KO or ITK-KO CAR-T cells via the lateral tail veins. For Raji cell-derived xenograft models, NPG mice were implanted with 5×10^5 Raji cells expressing

firefly luciferase intraperitoneally in the left flank. Ten days later, mice bearing tumor were intravenously injected with 5.0×10^6 nt-KO or ITK-KO CAR-T cells via the lateral tail veins. Following CAR-T cell injection, blood samples were collected from the orbital venous plexus of mice at indicated time points. Red blood cells were removed using ACK lysis buffer (Cat#A1049201, Gibco). Then PBMC cells were proceeded to flow cytometry analysis. Mice injected with MEC1 cells subcutaneously were monitored three times a week using a square caliper to measure tumor growth (tumor volume = π/6 × length × width × height) as previously described (67). Mice injected with MEC1 or Raji cells intraperitoneally or intravenously were monitored by in vivo imaging (IVIS Lumina III, PerkinElmer) at indicated timepoints. D-luciferin potassium salt (Cat #122799, PerkinElmer) was dissolved in PBS to create a working solution at 15 mg/mL. All mice received an intraperitoneal injection of luciferin solution (150mg/kg) 10 minutes prior to in vivo imaging.

Human T cell isolation and CAR-T production

Blood samples were obtained from the Second Xiangya Hospital. Ficoll-Paque (Cat#25710, Dongfang Huahui Co. Ltd., Beijing) was used for isolating peripheral blood mononuclear cells (PBMCs) as previously reported (68). PBMCs were further used for T cell enrichment using an EasySep Human T Cell Isolation Kit (Cat#17951, STEMCELL Technologies) following the manufacturer's instructions. The enriched T cells were activated with Dynabeads Human T-Activator CD3/CD28 (Cat#11132D, Gibco; T cells: beads = 1:2) for 24 hours and transduced with CAR-encoding lentivirus (multiplicity of infection (MOI) =8). Twenty-four hours after CAR transduction, the lentivirus-containing media was replaced with X-VIVO15 complete medium suppled with IL-2 (Peprotech, Cat#200-02, 100 U/mL). Gene editing in CAR-T cells by electroporation of RNP complex was performed 48 to 72 hours after CAR transduction. After gene editing, CAR-T cells were cultured for additional 3 to 5 days before proceeding with in vitro

analysis or further expansion, or for additional 11 to 14 days before injection into mice in the in vivo mouse experiments, unless otherwise noted.

Gene editing in CD19-CAR-T cells

CRISPR-mediated gene editing was used for deleting *ITK*. Single guide RNA (sgRNA) sequences were designed using the CRISPick online tool (https://portals.broadinstitute.org/gppx/crispick/public, Broad Institute) to achieve SpyCas9-mediated CRISPR-KO. Two sgRNAs (named ITK-sg1 and ITK-sg2, see Supplemental Table 1) were selected along with a non-targeting control sgRNA (named nt-sg1) (69), and synthesized (GenScript Co., Ltd. Nanjing, China). Cas9 protein was purchased from Advanced Biomart (Cat# CCN-066AB) and was delivered by nucleofection as a RNP complex with sgRNAs. Briefly, three days after CAR transduction, anti-CD3/CD28 beads were removed and 5×10^6 CAR-T cells were resuspended in 100µl electroporation buffer (P3 Primary Cell Solution 82µl mixed with Supplement 18µl; Cat#V4XP-3024, Lonza). Cas9 protein (30µg) was gently mixed with specific sgRNA (30µg) and placed at room temperature for 15 minutes, mixed with cells and transferred to Nucleocuvett Vessels and electroporated using a 4D-Nucleofactor (Cat#AAF-1003X, Lonza) with program EO115, followed by CAR-T cell culture and expansion in pre-warmed X-VIVO15 media. Three days later, genomic DNA was extracted and used for validation by Sanger sequencing. Gene-editing efficiency and potential off-target effects were validated by PCR (see Supplemental Table 1 and 2 respectively) and subsequently Sanger sequencing. The obtained sequencing results were analyzed with the TIDE online tool (http://shinyapps.datacurators.nl/tide/) to calculate gene editing efficiency, with a threshold set at a P-value of 0.001. SnapGene v6.01 was used for reading the Sanger sequencing results of DNA PCR products.

In vitro killing assay

MEC1 (CAT#CL-0761, Pricella), HG-3 (CAT#ACC765, DSMZ) and Raji cells (CAT#CL-0189, Pricella) stably expressing firefly luciferase were obtained via lentiviral transduction with the pLVX-Luc2-puro plasmid (Ningbo Testobio Co., Ltd (TSPLA10184)) following selection with 2 μg/ml puromycin (Cat# P8230, Solarbio, Beijing, China). CAR-T cells (effector, E) were co-cultured with tumor cells (target, T) at indicated ratios in a 96-well cell culture plate for 48 hours, and cancer cell lysis was detected using the Steady-Glo® Luciferase assay system (Cat#E2520, Promega). The percentage of specific lysis was calculated as:

$$\text{Specific lysis (\%)} = \left(1 - \left(\frac{value\ of\ test\ well - value\ of\ CAR{-}T\ cell\ only\ well}{value\ of\ tumor\ cell\ only\ well}\right)\right) \times 100\%$$

For serial tumor killing assays, CAR-T cells were co-cultured with MEC1 cells at an E: T ratio of 2:1 in a 96-well plate. Bioluminescence was measured every 48 hours and the E: T cell ratio was re-adjusted to 2:1 for co-culture after each sampling. Nine rounds of analyses were performed.

RNA sequencing and data analyses

CAR-T cells were co-cultured with MEC1 cells at an Effector (E) to target (T) ratio of 2:1 in X-VIVO 15 medium with 5% FBS at 37°C with 5% CO_2 for 48 hours. Following incubation, GFP^+ CAR-T cells were FACS-sorted and the purified nt-KO or ITK-KO CAR-T cells were used for both bulk and single cell RNA sequencing and analyses as previously described (70) and detailed in the Supplemental Materials. Sequencing data is available in NCBI.

Statistical analyses

Two-tailed unpaired Student's *t*-test was performed for statistical analysis by GraphPad Prism 6.01 software unless otherwise noted. Log-rank (Mantel-Cox) test with Bonferroni's correction for multiple comparisons was performed for the statistical analysis of the survival curves with Graphpad Prism 6.01 software. Statistical analyses of solid tumor growth in mouse model with subcutaneous injection of MEC1 cells were conducted by linear mixed-effect modeling (over the

whole-time course) with Bonferroni's correction for multiple comparisons as described previously (71). Data for statistical analyses were presented as mean ± SD unless otherwise noted. *, $P < 0.05$. **, $P < 0.01$. ***, $P < 0.001$. ****, $P < 0.0001$.

Study approval

All animal experiments were approved by the Institutional Animal Care and Use Committee of the Second Xiangya Hospital and the Suzhou Institute of Systems Medicine, Chinese Academy of Medical Sciences (CAMS-ISM) animal facility. This study involves human samples and was approved by the Institutional Review Board at the Second Xiangya Hospital (Reference number: 052 (2018)). Participants in the study gave informed consent in accordance with the Declaration of Helsinki before taking part.

Data availability

The bulk RNA-seq and scRNA-seq data in this study have been deposited in the NCBI database under accession code GSE278601 and GSE278612, respectively. Values for data points in figures are reported in the Supporting Data Values file. Other data and materials are available upon reasonable request.

Author contributions

WH and ZF conceived the research idea. ZF, HP, and WH designed the study. HP, ZF, QS and WH supervised this study. ZF, ZH, HX, QL, JL, YD, HZ, PW, HL, LH, YF, CW and KS acquired the data. ZH, HX, QS, SKC, KY, AZ, KS, WH and ZF analyzed the data. ZF, WH, HP, QS, ZH, AA, GV, AZ and KS prepared the manuscript. ZF was listed first among the co-first authors because ZF was responsible for all experimental designs, performed the animal experiments, analyzed and interpreted data, and drafted and revised the manuscript. ZH was listed second among the co-first authors because ZH participated in all the research, collected, analyzed, and

interpreted data, and revised the manuscript.

Acknowledgements

Z.H. was supported by the Scientific Research Launch Project for new employees of the Second Xiangya Hospital of Central South University and the Natural Science Foundation of. Hunan Province, China (2024JJ6557). H.P. was supported by the National Natural Science Foundation of China (82070175). Q.S. is supported by the CAMS Innovation Fund for Medical Sciences (2022-I2M-1-024, 2022-I2M-2-004, 2021-I2M-1-047), the NCTIB Fund for R&D Platform for Cell and Gene Therapy (ISM-2023-PT001) and Suzhou Municipal Key Laboratory (SZS2023005). W.H. and G.V. received support from the National Institutes of Health (R21 CA283872), the Center for Pre-Clinical Cancer Research funded by the National Institutes of Health (P20 GM135000), and the joint program of LSU Center for Comparative Oncology & Louisiana Children's Medical Center Cancer Center. A.A. received support from the National Institutes of Health (R01 AI120701 and AI138570). We are grateful to all the patients who participated in this study. We would like to thank Dr. Yi Liao from Xiamen University and Dr. Minxue Shen from Central South University for the help of statistical analyses, and Dr. Lianjun Zhang from CAMS-ISM for the helpful suggestions for the project. We thank Mr. Qingyuan He from CAMS-ISM animal facility for the help of animal services for several mouse experiments.

References

1. Cappell KM, and Kochenderfer JN. Long-term outcomes following CAR T cell therapy: what we know so far. *Nat Rev Clin Oncol.* 2023;20(6):359-71.
2. Hou AJ, Chen LC, and Chen YY. Navigating CAR-T cells through the solid-tumour microenvironment. *Nat Rev Drug Discov.* 2021;20(7):531-50.
3. Mackensen A, Muller F, Mougiakakos D, Boltz S, Wilhelm A, Aigner M, et al. Anti-CD19 CAR T cell therapy for refractory systemic lupus erythematosus. *Nat Med.* 2022;28(10):2124-32.
4. Schett G, Mackensen A, and Mougiakakos D. CAR T-cell therapy in autoimmune diseases. *Lancet.* 2023.
5. Rurik JG, Tombacz I, Yadegari A, Mendez Fernandez PO, Shewale SV, Li L, et al. CAR T cells produced in vivo to treat cardiac injury. *Science.* 2022;375(6576):91-6.
6. Gu T, Zhu M, Huang H, and Hu Y. Relapse after CAR-T cell therapy in B-cell malignancies: challenges and future approaches. *J Zhejiang Univ Sci B.* 2022;23(10):793-811.
7. Abramson JS. Post-CAR relapse in DLBCL: a fork in the road. *Blood.* 2022;140(24):2527-9.
8. Di Blasi R, Le Gouill S, Bachy E, Cartron G, Beauvais D, Le Bras F, et al. Outcomes of patients with aggressive B-cell lymphoma after failure of anti-CD19 CAR T-cell therapy: a DESCAR-T analysis. *Blood.* 2022;140(24):2584-93.
9. Amini L, Silbert SK, Maude SL, Nastoupil LJ, Ramos CA, Brentjens RJ, et al. Preparing for CAR T cell therapy: patient selection, bridging therapies and lymphodepletion. *Nat Rev Clin Oncol.* 2022;19(5):342-55.
10. Chong EA, Melenhorst JJ, Lacey SF, Ambrose DE, Gonzalez V, Levine BL, et al. PD-1 blockade modulates chimeric antigen receptor (CAR)-modified T cells: refueling the CAR. *Blood.* 2017;129(8):1039-41.
11. Zheng Y, Wang L, Yin L, Yao Z, Tong R, Xue J, et al. Lung Cancer Stem Cell Markers as Therapeutic Targets: An Update on Signaling Pathways and Therapies. *Front Oncol.* 2022;12:873994.
12. Chen J, Lopez-Moyado IF, Seo H, Lio CJ, Hempleman LJ, Sekiya T, et al. NR4A transcription factors limit CAR T cell function in solid tumours. *Nature.* 2019;567(7749):530-4.
13. Kong W, Dimitri A, Wang W, Jung IY, Ott CJ, Fasolino M, et al. BET bromodomain protein inhibition reverses chimeric antigen receptor extinction and reinvigorates exhausted T cells in chronic lymphocytic leukemia. *J Clin Invest.* 2021;131(16).
14. Mai D, Johnson O, Reff J, Fan TJ, Scholler J, Sheppard NC, et al. Combined disruption of T cell inflammatory regulators Regnase-1 and Roquin-1 enhances antitumor activity of engineered human T cells. *Proc Natl Acad Sci U S A.* 2023;120(12):e2218632120.
15. Tang N, Cheng C, Zhang X, Qiao M, Li N, Mu W, et al. TGF-beta inhibition via CRISPR promotes the long-term efficacy of CAR T cells against solid tumors. *JCI Insight.* 2020;5(4).
16. Prinzing B, Zebley CC, Petersen CT, Fan Y, Anido AA, Yi Z, et al. Deleting DNMT3A in CAR T cells prevents exhaustion and enhances antitumor activity. *Sci Transl Med.* 2021;13(620):eabh0272.

17. Wu L, Brzostek J, Sakthi Vale PD, Wei Q, Koh CKT, Ong JXH, et al. CD28-CAR-T cell activation through FYN kinase signaling rather than LCK enhances therapeutic performance. *Cell Rep Med.* 2023;4(2):100917.
18. Weber EW, Parker KR, Sotillo E, Lynn RC, Anbunathan H, Lattin J, et al. Transient rest restores functionality in exhausted CAR-T cells through epigenetic remodeling. *Science.* 2021;372(6537).
19. Mestermann K, Giavridis T, Weber J, Rydzek J, Frenz S, Nerreter T, et al. The tyrosine kinase inhibitor dasatinib acts as a pharmacologic on/off switch for CAR T cells. *Sci Transl Med.* 2019;11(499).
20. Weber EW, Lynn RC, Sotillo E, Lattin J, Xu P, and Mackall CL. Pharmacologic control of CAR-T cell function using dasatinib. *Blood Adv.* 2019;3(5):711-7.
21. Berg LJ. Strength of T cell receptor signaling strikes again. *Immunity.* 2009;31(4):529-31.
22. Andreotti AH, Schwartzberg PL, Joseph RE, and Berg LJ. T-cell signaling regulated by the Tec family kinase, Itk. *Cold Spring Harb Perspect Biol.* 2010;2(7):a002287.
23. Broussard C, Fleischacker C, Horai R, Chetana M, Venegas AM, Sharp LL, et al. Altered development of CD8+ T cell lineages in mice deficient for the Tec kinases Itk and Rlk. *Immunity.* 2006;25(1):93-104.
24. Hu J, Sahu N, Walsh E, and August A. Memory phenotype CD8+ T cells with innate function selectively develop in the absence of active Itk. *Eur J Immunol.* 2007;37(10):2892-9.
25. Huang W, Hu J, and August A. Cutting edge: innate memory CD8+ T cells are distinct from homeostatic expanded CD8+ T cells and rapidly respond to primary antigenic stimuli. *J Immunol.* 2013;190(6):2490-4.
26. Huang F, Huang W, Briggs J, Chew T, Bai Y, Deol S, et al. The tyrosine kinase Itk suppresses CD8+ memory T cell development in response to bacterial infection. *Scientific Reports.* 2015;5(1):7688.
27. Solouki S, Huang W, Elmore J, Limper C, Huang F, and August A. TCR Signal Strength and Antigen Affinity Regulate CD8(+) Memory T Cells. *J Immunol.* 2020;205(5):1217-27.
28. Huang W, Luo J, and August A. TCR/ITK signaling via mTOR tunes CD8⁺ T cell homeostatic proliferation, metabolism, and anti-tumor effector function. *bioRxiv.* 2018:359604.
29. Gill S, Vides V, Frey NV, Hexner EO, Metzger S, O'Brien M, et al. Anti-CD19 CAR T cells in combination with ibrutinib for the treatment of chronic lymphocytic leukemia. *Blood Adv.* 2022;6(21):5774-85.
30. Todorovic Z, Todorovic D, Markovic V, Ladjevac N, Zdravkovic N, Djurdjevic P, et al. CAR T Cell Therapy for Chronic Lymphocytic Leukemia: Successes and Shortcomings. *Curr Oncol.* 2022;29(5):3647-57.
31. Li L, Zhao M, Kiernan CH, Castro Eiro MD, van Meurs M, Brouwers-Haspels I, et al. Ibrutinib directly reduces CD8+T cell exhaustion independent of BTK. *Front Immunol.* 2023;14:1201415.
32. Bucks CM, Norton JA, Boesteanu AC, Mueller YM, and Katsikis PD. Chronic antigen stimulation alone is sufficient to drive CD8+ T cell exhaustion. *J Immunol.* 2009;182(11):6697-708.

33. Utzschneider DT, Alfei F, Roelli P, Barras D, Chennupati V, Darbre S, et al. High antigen levels induce an exhausted phenotype in a chronic infection without impairing T cell expansion and survival. *J Exp Med.* 2016;213(9):1819-34.
34. Zhao M, Li L, Kiernan CH, Castro Eiro MD, Dammeijer F, van Meurs M, et al. Overcoming immune checkpoint blockade resistance in solid tumors with intermittent ITK inhibition. *Sci Rep.* 2023;13(1):15678.
35. Riches JC, Davies JK, McClanahan F, Fatah R, Iqbal S, Agrawal S, et al. T cells from CLL patients exhibit features of T-cell exhaustion but retain capacity for cytokine production. *Blood.* 2013;121(9):1612-21.
36. Kalbasi A, Siurala M, Su LL, Tariveranmoshabad M, Picton LK, Ravikumar P, et al. Potentiating adoptive cell therapy using synthetic IL-9 receptors. *Nature.* 2022;607(7918):360-5.
37. Poorebrahim M, Melief J, Pico de Coaña Y, L. Wickström S, Cid-Arregui A, and Kiessling R. Counteracting CAR T cell dysfunction. *Oncogene.* 2021;40(2):421-35.
38. Daniels KG, Wang S, Simic MS, Bhargava HK, Capponi S, Tonai Y, et al. Decoding CAR T cell phenotype using combinatorial signaling motif libraries and machine learning. *Science.* 2022;378(6625):1194-200.
39. Castellanos-Rueda R, Di Roberto RB, Bieberich F, Schlatter FS, Palianina D, Nguyen OTP, et al. speedingCARs: accelerating the engineering of CAR T cells by signaling domain shuffling and single-cell sequencing. *Nat Commun.* 2022;13(1):6555.
40. Bertilaccio MT, Scielzo C, Simonetti G, Ponzoni M, Apollonio B, Fazi C, et al. A novel Rag2-/-gammac-/--xenograft model of human CLL. *Blood.* 2010;115(8):1605-9.
41. Paggetti J, Haderk F, Seiffert M, Janji B, Distler U, Ammerlaan W, et al. Exosomes released by chronic lymphocytic leukemia cells induce the transition of stromal cells into cancer-associated fibroblasts. *Blood.* 2015;126(9):1106-17.
42. Bai Y, Kan S, Zhou S, Wang Y, Xu J, Cooke JP, et al. Enhancement of the in vivo persistence and antitumor efficacy of CD19 chimeric antigen receptor T cells through the delivery of modified TERT mRNA. *Cell Discov.* 2015;1:15040.
43. Wen H, Lou X, Qu Z, Qin C, Jiang H, Yang Y, et al. Pre-clinical efficacy of CD20-targeted chimeric antigen receptor T cells for non-Hodgkin's lymphoma. *Discover Oncology.* 2022;13(1):122.
44. Dubovsky JA, Beckwith KA, Natarajan G, Woyach JA, Jaglowski S, Zhong Y, et al. Ibrutinib is an irreversible molecular inhibitor of ITK driving a Th1-selective pressure in T lymphocytes. *Blood.* 2013;122(15):2539-49.
45. Sterner RC, and Sterner RM. CAR-T cell therapy: current limitations and potential strategies. *Blood Cancer J.* 2021;11(4):69.
46. Cornberg M, Kenney LL, Chen AT, Waggoner SN, Kim SK, Dienes HP, et al. Clonal exhaustion as a mechanism to protect against severe immunopathology and death from an overwhelming CD8 T cell response. *Front Immunol.* 2013;4:475.
47. Heyman BM, Tzachanis D, and Kipps TJ. Recent Advances in CAR T-Cell Therapy for Patients with Chronic Lymphocytic Leukemia. *Cancers (Basel).* 2022;14(7).
48. Kapnick SM, Stinchcombe JC, Griffiths GM, and Schwartzberg PL. Inducible T Cell Kinase Regulates the Acquisition of Cytolytic Capacity and Degranulation in CD8(+) CTLs. *J Immunol.* 2017;198(7):2699-711.

49. Huang W, and August A. The signaling symphony: T cell receptor tunes cytokine-mediated T cell differentiation. *J Leukoc Biol.* 2015;97(3):477-85.
50. Smith GA, Taunton J, and Weiss A. IL-2Rbeta abundance differentially tunes IL-2 signaling dynamics in CD4(+) and CD8(+) T cells. *Sci Signal.* 2017;10(510).
51. Lynn RC, Weber EW, Sotillo E, Gennert D, Xu P, Good Z, et al. c-Jun overexpression in CAR T cells induces exhaustion resistance. *Nature.* 2019;576(7786):293-300.
52. Mount CW, Majzner RG, Sundaresh S, Arnold EP, Kadapakkam M, Haile S, et al. Potent antitumor efficacy of anti-GD2 CAR T cells in H3-K27M(+) diffuse midline gliomas. *Nat Med.* 2018;24(5):572-9.
53. Larson RC, Kann MC, Bailey SR, Haradhvala NJ, Llopis PM, Bouffard AA, et al. CAR T cell killing requires the IFNgammaR pathway in solid but not liquid tumours. *Nature.* 2022;604(7906):563-70.
54. Wang D, Prager BC, Gimple RC, Aguilar B, Alizadeh D, Tang H, et al. CRISPR Screening of CAR T Cells and Cancer Stem Cells Reveals Critical Dependencies for Cell-Based Therapies. *Cancer Discov.* 2021;11(5):1192-211.
55. Shaul O. How introns enhance gene expression. *Int J Biochem Cell Biol.* 2017;91(Pt B):145-55.
56. Eken A, Cansever M, Somekh I, Mizoguchi Y, Zietara N, Okus FZ, et al. Genetic Deficiency and Biochemical Inhibition of ITK Affect Human Th17, Treg, and Innate Lymphoid Cells. *J Clin Immunol.* 2019;39(4):391-400.
57. Gomez-Rodriguez J, Sahu N, Handon R, Davidson TS, Anderson SM, Kirby MR, et al. Differential expression of interleukin-17A and -17F is coupled to T cell receptor signaling via inducible T cell kinase. *Immunity.* 2009;31(4):587-97.
58. Elmore J, Carter C, Redko A, Koylass N, Bennett A, Mead M, et al. ITK independent development of Th17 responses during hypersensitivity pneumonitis driven lung inflammation. *Commun Biol.* 2022;5(1):162.
59. Mamontov P, Eberwine RA, Perrigoue J, Das A, Friedman JR, and Mora JR. A negative role for the interleukin-2-inducible T-cell kinase (ITK) in human Foxp3+ TREG differentiation. *PLoS One.* 2019;14(4):e0215963.
60. Mammadli M, Harris R, Suo L, May A, Gentile T, Waickman AT, et al. Interleukin-2-inducible T-cell kinase (Itk) signaling regulates potent noncanonical regulatory T cells. *Clin Transl Med.* 2021;11(12):e625.
61. Miller AT, Wilcox HM, Lai Z, and Berg LJ. Signaling through Itk promotes T helper 2 differentiation via negative regulation of T-bet. *Immunity.* 2004;21(1):67-80.
62. Kosaka Y, Felices M, and Berg LJ. Itk and Th2 responses: action but no reaction. *Trends Immunol.* 2006;27(10):453-60.
63. Fischer AM, Mercer JC, Iyer A, Ragin MJ, and August A. Regulation of CXC chemokine receptor 4-mediated migration by the Tec family tyrosine kinase ITK. *J Biol Chem.* 2004;279(28):29816-20.
64. Takesono A, Horai R, Mandai M, Dombroski D, and Schwartzberg PL. Requirement for Tec kinases in chemokine-induced migration and activation of Cdc42 and Rac. *Curr Biol.* 2004;14(10):917-22.

65. Cho HS, Ha S, Shin HM, Reboldi A, Hall JA, Huh JR, et al. CD8(+) T Cells Require ITK-Mediated TCR Signaling for Migration to the Intestine. *Immunohorizons.* 2020;4(2):57-71.
66. Kannan AK, Kim DG, August A, and Bynoe MS. Itk signals promote neuroinflammation by regulating CD4+ T-cell activation and trafficking. *J Neurosci.* 2015;35(1):221-33.
67. Wang H, Hu S, Chen X, Shi H, Chen C, Sun L, et al. cGAS is essential for the antitumor effect of immune checkpoint blockade. *Proc Natl Acad Sci U S A.* 2017;114(7):1637-42.
68. Grievink HW, Luisman T, Kluft C, Moerland M, and Malone KE. Comparison of Three Isolation Techniques for Human Peripheral Blood Mononuclear Cells: Cell Recovery and Viability, Population Composition, and Cell Functionality. *Biopreserv Biobank.* 2016;14(5):410-5.
69. Ting PY, Parker AE, Lee JS, Trussell C, Sharif O, Luna F, et al. Guide Swap enables genome-scale pooled CRISPR-Cas9 screening in human primary cells. *Nat Methods.* 2018;15(11):941-6.
70. Shan Q, Zeng Z, Xing S, Li F, Hartwig SM, Gullicksrud JA, et al. The transcription factor Runx3 guards cytotoxic CD8(+) effector T cells against deviation towards follicular helper T cell lineage. *Nat Immunol.* 2017;18(8):931-9.
71. Enot DP, Vacchelli E, Jacquelot N, Zitvogel L, and Kroemer G. TumGrowth: An open-access web tool for the statistical analysis of tumor growth curves. *Oncoimmunology.* 2018;7(9):e1462431.

Figure Legends

Figure 1 ITK deficiency attenuates immediate cytotoxicity of CAR-T cells

Nt-KO indicates the control group of CAR-T cells electroporated with RNP complex containing non-targeting sgRNA, while ITK-KO indicates the group that received *ITK*-targeting sgRNA. (**A**) Schematic representation of the anti-human CD19-CAR molecule. CMV, cytomegalovirus promoter. CD8αSP, signal peptide of human CD8α. anti-CD19-scFv, single chain fragment variable of anti-human CD19 antibody (clone: FMC63). CD8αTM, transmembrane domain of human CD8α. CD28, 4-1BB and CD3ζ, signal transduction domains of human CD28, 4-1BB and CD3ζ, respectively. (**B**) Generation of ITK-deficient CAR-T cells. Briefly, T cells were enriched from PBMCs and activated with anti-CD3/CD28 beads for 24 hours. Then, T cells were transduced with CAR-encoding lentivirus. 48 hours post-transduction, CAR-T cells were electroporated with RNP complex. (**C**) Gene editing efficiency of *ITK* locus by sgRNA1 targeting *ITK* (ITK-sgRNA1). CAR-T cells were collected for analysis 3 days after electroporation of RNP complex. (**D**) Validation of *ITK* deficiency at protein level by western blotting. CAR-T cells were collected for western blotting 5 days after electroporation. (**E**-**G**) In vitro killing assay against the indicated target tumor cells using control and ITK-KO CAR-T cells (n = 4). Luciferase-expressing MEC1, HG3 and Raji cells were mixed at the indicated ratios with CAR-T cells and analyzed 48 hours after co-culture. (**H**) Representative flow cytometric plots of IFN-γ, TNF-α and Granzyme B expression in CAR-T cells stimulated as indicated. E, effector (CAR-T cells). T, target (MEC1 cells). (**I**) Summary of percentages of CAR-T cells expressing different cytokines in **H** (n = 4). Compiled data from one independent experiment for **E**-**G** and **I**. Technical replicates are shown in **E**-**G** and **I**. Data represent results of at least two independent experiments in **C**-**I.**

Figure 2 ITK deficiency promotes long-term expansion of CD19-CAR-T cell in vitro

(**A**-**C**) Fold expansion of total (**A**), $CD4^+$ (**B**) and $CD8^+$ (**C**) CD19-CAR-T cells at the indicated time

points, following 48 hours co-culture with MEC1 cells at the E:T ratio of 2:1 (n = 3). Fold expansion values of the cell numbers were normalized to the average cell number of the CD19-CAR-T cells at day 0. (**D** and **E**) Representative flow cytometric plots of Annexin V and 7-AAD (**D**) and summary of percentages of Annexin V^+ cells (**E**) in CAR-T cells at the indicated time points. (**F** and **G**) Representative flow cytometric plots of Ki-67 (**F**) and summary of percentages of Ki-67^+ cells (**G**) in CAR-T cells at the indicated time points. n = 3 for each group in **E** and **G**. Compiled data from one independent experiment in **A**-**C**, **E** and **G**. Data represent results of at least two independent experiments. Statistical differences were determined by two-tailed unpaired Student's *t*-test.

Figure 3 Transcriptomic regulation of CD19-CAR-T cells by ITK

CAR-T cells were co-cultured with MEC1 cells for 48 hours and sort-purified for both bulk and single-cell RNA sequencing (RNA-Seq). (**A**-**E**) Bulk RNA-seq analysis of the transcriptome in nt-KO and ITK-KO CAR-T cells. (**A**) Differential gene expression (TPM ≥ 1, P ≤ 0.05, fold change ≥ 1.5). Unadjusted P values are shown. (**B**) KEGG analysis of the differentially expressed genes. (**C**) Heatmap of the indicated gene expression. (**D**) RNA-seq tracks of read coverage at the *TCF7* (left), *KLF2* (middle) and *LAG3* (right) loci in CAR-T cells. (**E**) Gene set enrichment analysis (GSEA) of the Effector-memory CD8 T cell gene set analysis using differentially expressed genes shown in **A**. (**F**-**K**) Single-cell RNA-seq (scRNA-seq) analysis of the transcriptome in nt-KO and ITK-KO CAR-T cells. (**F**) Clustering of functional T cell subsets of all CAR-T cells based on UMAP. (**G**) Percentage of indicated T cell subsets within total T cells identified by scRNA-seq in **F**. (**H**-**K**) Expression of indicated genes in nt-KO and ITK-KO CD19-CAR-T cells.

Figure 4 ITK deficiency reduces exhaustion and promote memory phenotype in CD19-CAR-T cells in vitro

CAR-T cells were co-cultured with MEC1 following the serial killing assay protocol detailed in the

method section. (**A**) Representative flow cytometric plots of CD69 expression in the indicated CAR-T cells in the presence or absence of MEC1 cells. CAR-T cells were analyzed after co-culture with MEC1 cells (E:T = 2:1) for 48 hours. (**B**) Summary of percentages of $CD69^+$ cells in **A** (n = 3 for each CAR-T only group, and n = 4 for each CAR-T + MEC1 group) (two-way ANOVA with Sidak correction for multiple comparisons; *, P < 0.05; ****, P < 0.0001). (**C**) Representative flow cytometric plots of PD-1, TIGIT, TIM-3 and CTLA4 expression in CAR-T cells 15 days after co-culture with MEC1 cells at the ratio of E:T = 2:1. (**D**) Summary of percentages of $PD\text{-}1^+$, $TIGTI^+$, $TIM\text{-}3^+$, and $CTLA4^+$ cells as shown in **C** (n = 4)**.** (**E**). Summary of percentages of $LAG\text{-}3^+$, $PD\text{-}1^+$ and $TIM\text{-}3^+$ cells in the indicated CAR-T cells following the indicated rounds of co-culture with MEC1 cells (n = 4). CAR-T cells were co-cultured with MEC1 cells at 2:1 ratio for 48 hours for each round for **E** and **F**. (**F**) Percentages of specific lysis determined by in vitro killing assay of MEC1 cells by the indicated CAR-T cells at indicated rounds of co-culture (n = 4). (**G**) Representative flow cytometric plots of CD45RA and CCR7 expression the in indicated CAR-T cells 15 days after co-culture with MEC1 cells (E:T = 2:1). (**H**) Summary of percentages of CAR-T cells expressing CD45RA and/or CCR7 in **G** (n = 3). Compiled data from one independent experiment for **B**, **D**-**F** and **H**. Two-tailed unpaired Student's *t*-test in **D**-**F** and **H**. Data represent results of at least two independent experiments.

Figure 5 *ITK* deficiency enhances expansion and long-term persistence of CD19-CAR-T cells in vivo

(**A**) Experimental design of the CAR-T therapy against intraperitoneally (i.p.) injected MEC1 in NPG mice. CAR-T cells were expanded for 11 days after electroporation before i.v. injection into mice. PB, peripheral blood. (**B**) Representative flow cytometric plots of CAR-GFP and CD3 in the PB samples collected from nt-KO or ITK-KO CD19-CAR-T cell recipients at the indicated time points. (**C**) Summary of the percentages of CAR-T cells ($CD3^+GFP^+$) showed in **B** (n = 3 for day 77 ITK-KO group and n = 4 for the rest). (**D**) Representative flow cytometric plots of the indicated

molecules by CAR-T cells in the PB samples collected from nt-KO or ITK-KO-CAR recipients 28 days after CAR-T cell infusion. (**E**) Summary of the percentages of CAR-T cells that are LAG-3$^+$, PD-1$^+$, TIM-3$^+$, TIGIT$^+$, or CTLA-4$^+$, as shown in **D** (n = 4). (**F** and **G**) Summary of the percentages of CAR-T cells that are Ki-67$^+$ (**F**) and Annexin V$^+$ (**G**) as shown in **Supplemental Figure 5, C** and **D** (n = 5). (**H**) Statistical analysis of different populations of cells shown in **Supplemental Figure 5E** (n = 4). (**I**) Experimental design of the CAR-T therapy against subcutaneously (s.c.) injected MEC1 in NPG mice. CAR-T cells were expanded for 11 days after electroporation before i.v. injection into mice. (**J**) Representative flow cytometric plots of CAR-GFP and CD3 in the PB samples collected from nt-KO or ITK-KO CD19-CAR recipients at the indicated time points. (**K**) Summary of the percentages of CAR-T cells (CD3$^+$GFP$^+$) showed in **J** (n = 4, mean ± SEM). Compiled data from one independent experiment for **C**, **E**-**H** and **K**. Statistical differences were determined by two-tailed unpaired Student's *t*-test. Data represent results of at least two independent experiments.

Figure 6 ITK-deficient CAR-T cells significantly improve control of tumor relapse in vivo (**A**) Experimental design of the CAR-T therapy against intraperitoneally (i.p.) injected Raji in NPG mice. CAR-T cells were expanded for 11 days after electroporation before i.v. injection into mice. (**B**) Representative flow cytometric plots of CAR-GFP and CD3 in the PB samples collected from indicated recipients at the indicated time points. (**C**) Summary of the percentages of CAR-T cells (CD3$^+$GFP$^+$) showed in **B** (n = 1 for day 95 nt-KO group, n = 3 for day 95 ITK-KO group, n = 4 for the rest). (**D**) Representative flow cytometric plots of Annexin V and 7-AAD by CAR-T cells in the PB samples collected from indicated recipients 28 days after CAR-T cell injection. (**E**) Summary of the percentages of CAR-T cells that are Annexin V$^+$ as shown in **D** (n = 4). (**F**) Representative flow cytometric plots of LAG-3 and TIGIT expression by CAR-T cells in the PB samples collected from indicated recipients 24 days after CAR-T cell infusion. (**G**) Summary of the percentages of CAR-T cells that are LAG-3$^+$ or TIGIT$^+$, as shown in **F** (n = 4). (**H**) Representative bioluminescence

images of NPG mice xenografted with Raji cells as designed in **A**. Representative figures from one independent experiment. Experiment was repeated twice. (**I**) Kaplan-Meier survival of Raji-bearing NPG mice treated with PBS, nt-KO CAR-T or ITK-KO CAR-T cells (n = 9) (log-rank Mantel-Cox test with Bonferroni's correction for multiple comparisons; **, $P < 0.01$; ****, $P < 0.0001$). Compiled data from two independent experiments. (**J**) Statistical analysis of CD45RO and/or CCR7 expression by CAR-T cells shown in **Supplemental Figure 6G** (n = 4). (**K**) Statistical analysis of ratio of Raji to CAR-T cells as shown in **Supplemental Figure 6H** (n = 4). (**M**) Statistical analysis of fold change of CAR-T cell numbers in samples as shown in **Supplemental Figure 6H** (n = 4). (**N**) Statistical analysis of percentage of IFN-γ, TNF-α and Granzyme B expression in CAR-T cells shown in **Supplemental Figure 6I** (n = 3). Compiled data from one independent experiment for **C**, **E**, **G**, **J** and **K**-**M**. Two-tailed unpaired Student's *t*-test was performed in **C**, **E**, **G**, **J** and **K**-**M**. Data represent results of at least two independent experiments.

Figure 7 ITK deficiency attenuates exhaustion and promotes memory phenotype in CD19-CAR-T cells derived from CLL patients

(**A**) Flow cytometric analyses of IFN-γ, TNF-α, and Granzyme B expression in CLL-CAR-T cells. CLL-CAR-T cells were co-cultured with MEC1 cells at a 2:1 ratio for 48 hours in **A**-**J**. (**B**) Statistical analysis of the percentage of IFN-γ, TNF-α, and Granzyme B expression in CAR-T cells shown in **A** (n = 5). (**C**) Flow cytometry analyses of CD69 expression in indicated CLL-CAR-T cells after co-culture with or without MEC1 cells. (**D**) Statistical analysis of CD69 expression shown in **C** (n = 3 for CAR-T only group, n = 4 for CAR-T + MEC1 group). (**E**) Flow cytometry analyses of LAG-3, PD-1, and TIM-3 expression in indicated CLL-CAR-T cells. (**F**) Statistical analysis of the percentage of LAG-3$^+$, PD-1$^+$, and TIM-3$^+$ cells shown in **E** (n = 3 for CAR-T only group, n = 4 for CAR-T + MEC1 group). (**G**) Flow cytometry analyses of Annexin V and 7-AAD expression in indicated CLL-CAR-T cells at indicated time points. (**H**) Statistical analysis of Annexin V$^+$ CAR-T

cells shown in **G** (n = 4). (**I**) Flow cytometry analyses of CD69, LAG-3, and PD-1 expression in indicated CAR-T cells co-cultured with MEC1 cells with/without PF-06465469 (1 μM) treatment. (**J**) Statistical analysis of the percentage of $CD69^+$, $LAG\text{-}3^+$, and $PD\text{-}1^+$ cells in CD19-CAR-T cells shown in **I** (n = 4). (**K**) Representative flow cytometric plots of CD45RA and CCR7 expression in indicated CAR-T cells 15 days after PF-06465469 treatment. (**L**) Summary of percentages of CAR-T cells expressing CD45RA and/or CCR7 in **K** (n = 4). Compiled data from one independent experiment for **B**, **D**, **F**, **H**, **J** and **L**. Statistical differences were determined by two-tailed unpaired Student's *t*-test. Data represent results of at least two independent experiments.

Figure 8 ITK-deficient CAR-T cells derived from CLL patients improve control of tumor relapse in vivo

(**A**) Experimental design of the CAR-T therapy against intravenously injected MEC1 cells expressing luciferase in NPG mice via the lateral tail veins. CAR-T cells were expanded for 12 days following electroporation before i.v. injection into mice. (**B**) Representative flow cytometric plots of CAR-GFP and CD3 in the PBMCs collected from CLL-CAR-T cell recipients at the indicated time points. (**C**) Summary of the percentages of CAR-T cells ($CD3^+GFP^+$) as shown in **B** (mean ± SEM. n = 5 for the nt-KO groups on day 26, 33, and 40, as well as the ITK-KO groups on day 40 and 52. n=4 for nt-KO day 52 group. n = 6 for the rest groups). (**D**) Representative flow cytometric plots of TIM-3 expression on CAR-T cells in the PBMCs collected from nt-KO or ITK-KO CLL-CAR-T recipients 26 days post-infusion. (**E**) Summary of the percentages of CAR-T cells that are $TIM\text{-}3^+$ as shown in **D** (n = 5). (**F**) Representative flow cytometric plots of CD62L and CD45RA expression in the indicated CAR-T cells collected. PBMCs were collected on day 33 after CAR-T cell injection. (**G**) Statistical analysis of different cell populations as shown in **F** (n = 5). (**H**) Representative bioluminescence images of NPG mice xenografted with MEC1 cells as designed in **A**. (**I**) Survival of MEC1-bearing NPG mice treated with PBS, nt-KO CLL-CAR-T or ITK-KO CLL-CAR-T cells (n = 6) (log-rank Mantel-Cox test with Bonferroni's correction for multiple

965 comparisons; *, P < 0.05; **, P < 0.01). Compiled data from two independent experiments in **C**,
966 **E**, **G** and **I**. Statistical differences were determined by two-tailed unpaired Student's *t*-test in **C**, **E**
967 and **G**. Data represent results of two independent experiments.

Figure 1

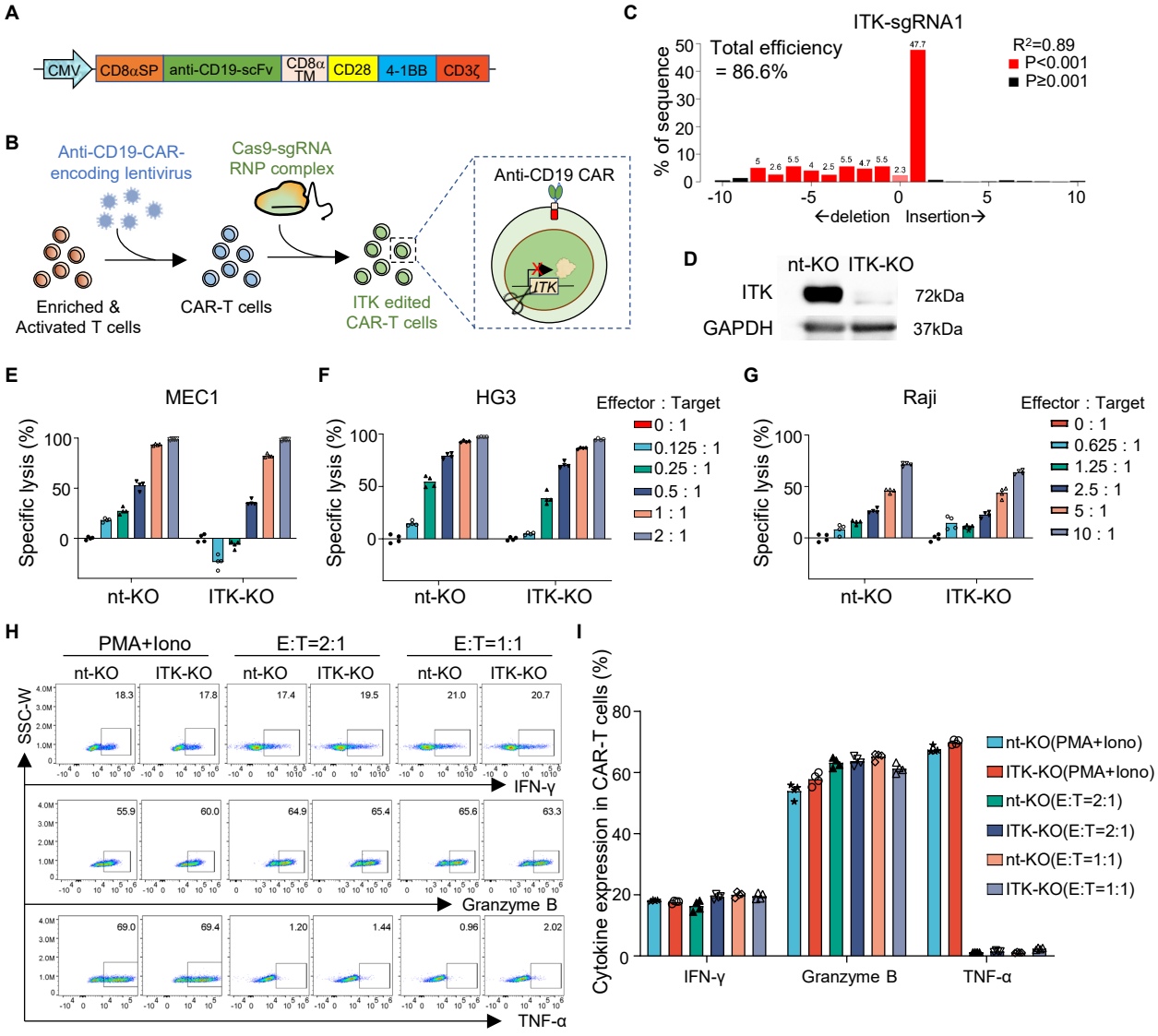
A
CMV
CD8αSP
anti-CD19-scFv
CD8α TM
CD28
4-1BB
CD3ζ
B
Anti-CD19-CAR-encoding lentivirus
Cas9-sgRNA RNP complex
Anti-CD19 CAR
ITK
Enriched & Activated T cells
CAR-T cells
ITK edited CAR-T cells
C
ITK-sgRNA1
Total efficiency = 86.6%
R²=0.89
P<0.001
P≥0.001
% of sequence
←deletion Insertion→
D
nt-KO ITK-KO
ITK
GAPDH
72kDa
37kDa
E
MEC1
Specific lysis (%)
nt-KO
ITK-KO
F
HG3
Effector : Target
0 : 1
0.125 : 1
0.25 : 1
0.5 : 1
1 : 1
2 : 1
G
Raji
0 : 1
0.625 : 1
1.25 : 1
2.5 : 1
5 : 1
10 : 1
H
PMA+Iono
E:T=2:1
E:T=1:1
SSC-W
IFN-γ
Granzyme B
TNF-α
I
Cytokine expression in CAR-T cells (%)
nt-KO(PMA+Iono)
ITK-KO(PMA+Iono)
nt-KO(E:T=2:1)
ITK-KO(E:T=2:1)
nt-KO(E:T=1:1)
ITK-KO(E:T=1:1)
IFN-γ
Granzyme B
TNF-α

Figure 2

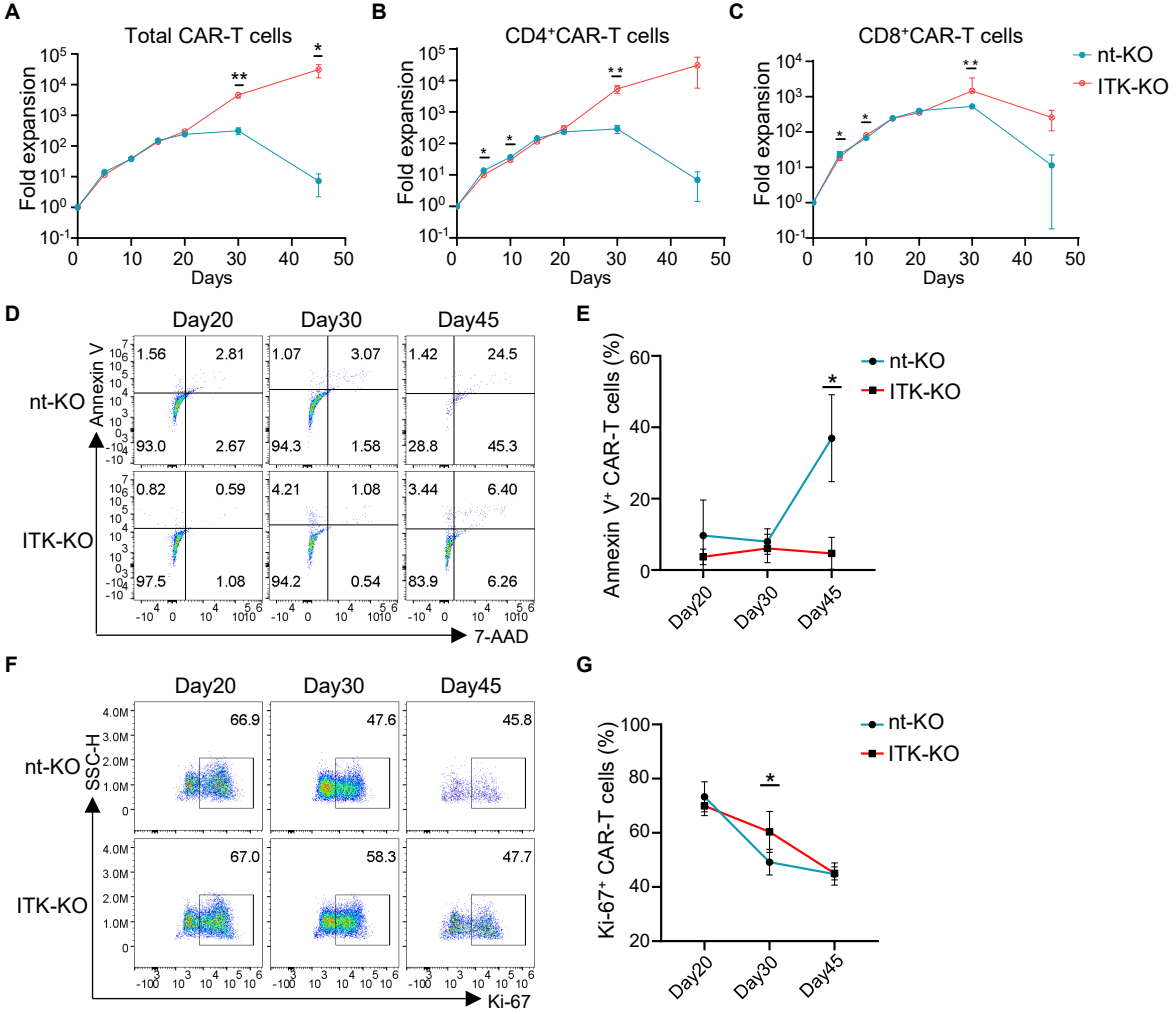
A
Total CAR-T cells
Fold expansion
Days
B
CD4⁺CAR-T cells
C
CD8⁺CAR-T cells
nt-KO
ITK-KO
D
Day20
Day30
Day45
nt-KO
ITK-KO
Annexin V
7-AAD
1.56
2.81
93.0
2.67
1.07
3.07
94.3
1.58
1.42
24.5
28.8
45.3
0.82
0.59
97.5
1.08
4.21
1.08
94.2
0.54
3.44
6.40
83.9
6.26
E
Annexin V⁺ CAR-T cells (%)
F
SSC-H
Ki-67
66.9
47.6
45.8
67.0
58.3
47.7
G
Ki-67⁺ CAR-T cells (%)

Figure 3

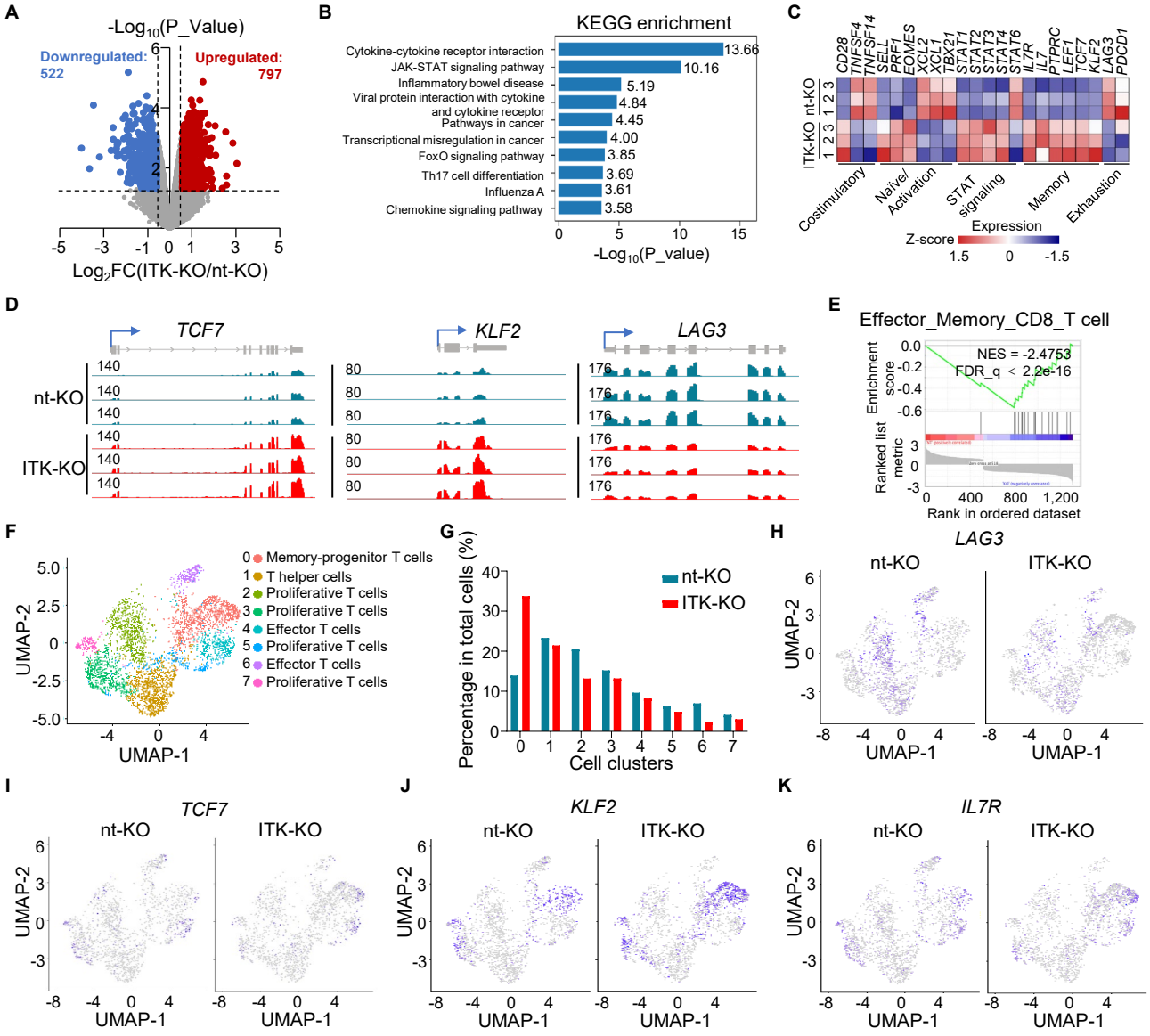
A
-Log10(P_Value)
Downregulated: 522
Upregulated: 797
Log2FC(ITK-KO/nt-KO)
B
KEGG enrichment
Cytokine-cytokine receptor interaction
JAK-STAT signaling pathway
Inflammatory bowel disease
Viral protein interaction with cytokine and cytokine receptor
Pathways in cancer
Transcriptional misregulation in cancer
FoxO signaling pathway
Th17 cell differentiation
Influenza A
Chemokine signaling pathway
13.66
10.16
5.19
4.84
4.45
4.00
3.85
3.69
3.61
3.58
-Log10(P_value)
C
CD28
TNFSF4
TNFSF14
SELL
PRF1
EOMES
XCL2
XCL1
TBX21
STAT1
STAT2
STAT3
STAT4
STAT6
IL7R
IL7
PTPRC
LEF1
TCF7
KLF2
LAG3
PDCD1
nt-KO
ITK-KO
Costimulatory
Naïve/ Activation
STAT signaling
Memory
Exhaustion
Expression
Z-score
D
TCF7
KLF2
LAG3
nt-KO
ITK-KO
E
Effector_Memory_CD8_T cell
NES = -2.4753
FDR_q < 2.2e-16
Enrichment score
Ranked list metric
Rank in ordered dataset
F
0 Memory-progenitor T cells
1 T helper cells
2 Proliferative T cells
3 Proliferative T cells
4 Effector T cells
5 Proliferative T cells
6 Effector T cells
7 Proliferative T cells
UMAP-1
UMAP-2
G
nt-KO
ITK-KO
Percentage in total cells (%)
Cell clusters
H
LAG3
nt-KO
ITK-KO
I
TCF7
J
KLF2
K
IL7R

Figure 4

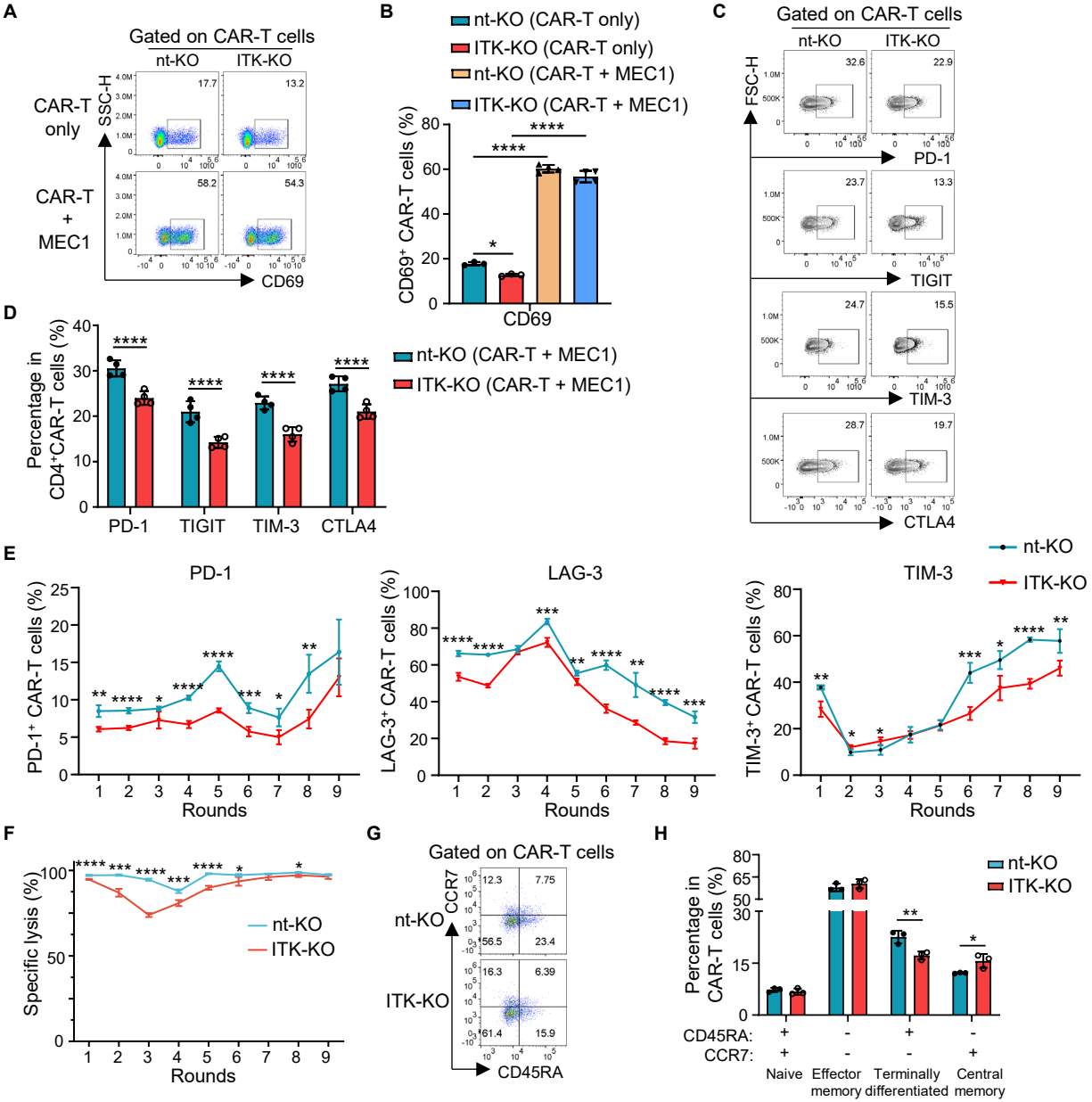
A
Gated on CAR-T cells
nt-KO
ITK-KO
CAR-T only
CAR-T + MEC1
SSC-H
CD69
17.7
13.2
58.2
54.3
B
nt-KO (CAR-T only)
ITK-KO (CAR-T only)
nt-KO (CAR-T + MEC1)
ITK-KO (CAR-T + MEC1)
CD69⁺ CAR-T cells (%)
CD69
C
Gated on CAR-T cells
nt-KO
ITK-KO
FSC-H
PD-1
TIGIT
TIM-3
CTLA4
32.6
22.9
23.7
13.3
24.7
15.5
28.7
19.7
D
Percentage in CD4⁺CAR-T cells (%)
PD-1
TIGIT
TIM-3
CTLA4
nt-KO (CAR-T + MEC1)
ITK-KO (CAR-T + MEC1)
E
PD-1⁺ CAR-T cells (%)
LAG-3⁺ CAR-T cells (%)
TIM-3⁺ CAR-T cells (%)
Rounds
nt-KO
ITK-KO
F
Specific lysis (%)
Rounds
nt-KO
ITK-KO
G
Gated on CAR-T cells
nt-KO
ITK-KO
CCR7
CD45RA
12.3
7.75
56.5
23.4
16.3
6.39
61.4
15.9
H
Percentage in CAR-T cells (%)
nt-KO
ITK-KO
CD45RA:
CCR7:
Naive
Effector memory
Terminally differentiated
Central memory

Figure 5

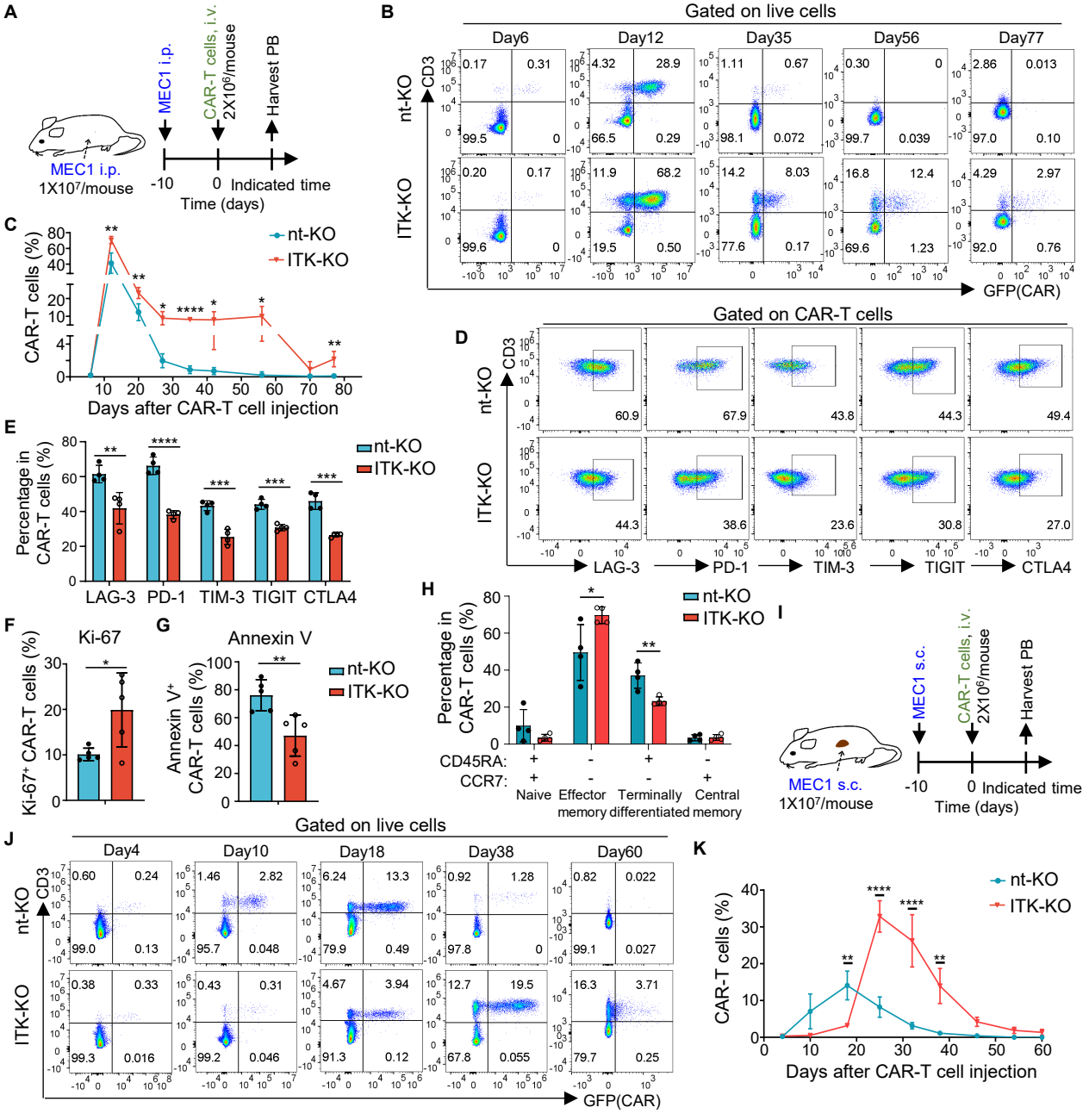
A
MEC1 i.p.
1X10⁷/mouse
MEC1 i.p.
CAR-T cells, i.v.
2X10⁶/mouse
Harvest PB
-10
0
Indicated time
Time (days)
B
Gated on live cells
Day6
Day12
Day35
Day56
Day77
nt-KO
ITK-KO
CD3
GFP(CAR)
C
CAR-T cells (%)
nt-KO
ITK-KO
Days after CAR-T cell injection
D
Gated on CAR-T cells
LAG-3
PD-1
TIM-3
TIGIT
CTLA4
E
Percentage in CAR-T cells (%)
F
Ki-67
Ki-67⁺ CAR-T cells (%)
G
Annexin V
Annexin V⁺ CAR-T cells (%)
H
CD45RA:
CCR7:
Naive
Effector memory
Terminally differentiated
Central memory
I
MEC1 s.c.
1X10⁷/mouse
J
Day4
Day10
Day18
Day38
Day60
K

Figure 6

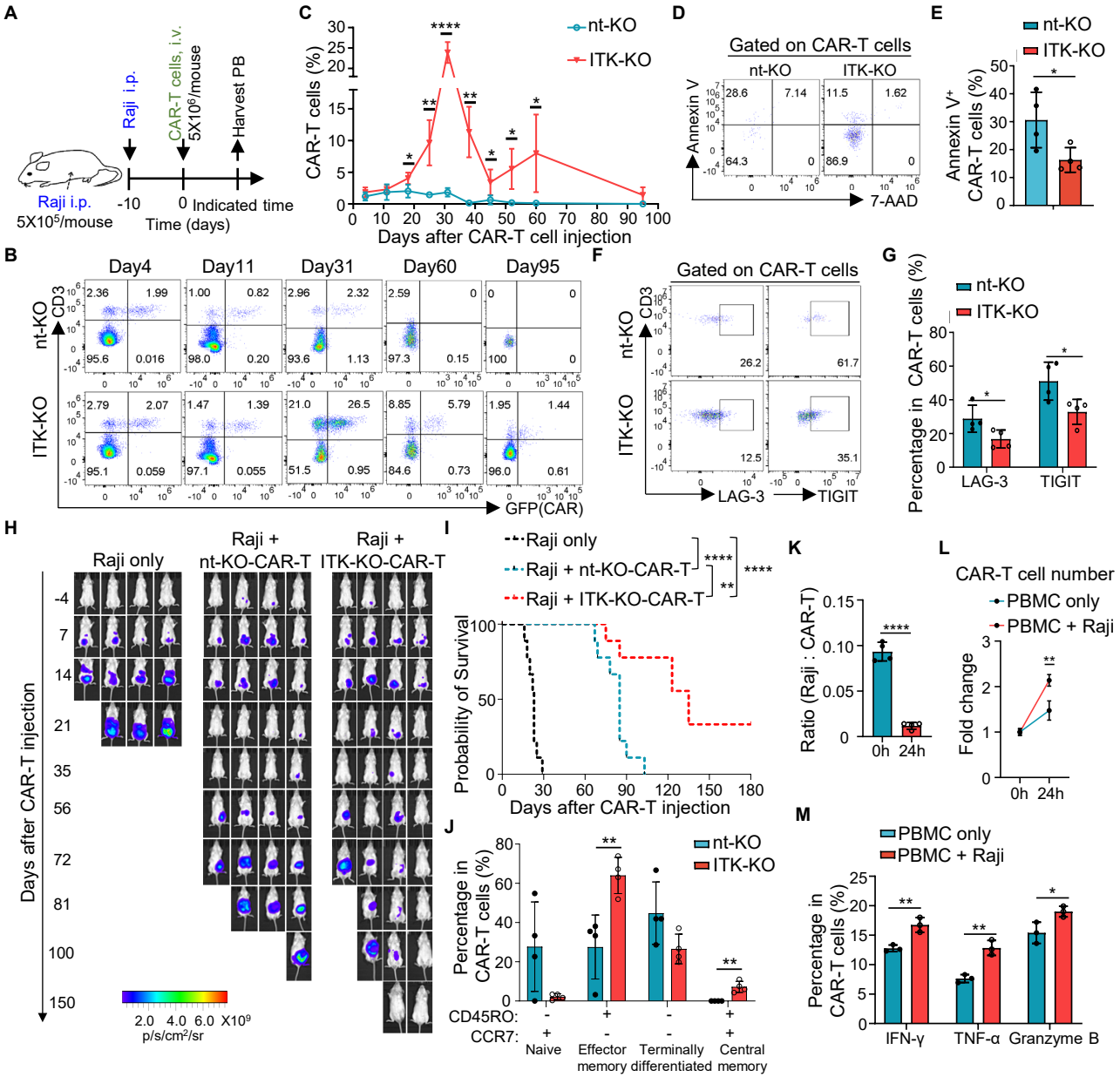
A
Raji i.p.
CAR-T cells, i.v.
5X10⁶/mouse
Harvest PB
Raji i.p.
5X10⁵/mouse
-10
0
Indicated time
Time (days)
C
nt-KO
ITK-KO
CAR-T cells (%)
Days after CAR-T cell injection
D
Gated on CAR-T cells
nt-KO
ITK-KO
Annexin V
7-AAD
E
nt-KO
ITK-KO
Annexin V⁺ CAR-T cells (%)
B
Day4
Day11
Day31
Day60
Day95
nt-KO
ITK-KO
CD3
GFP(CAR)
F
Gated on CAR-T cells
nt-KO
ITK-KO
CD3
LAG-3
TIGIT
G
nt-KO
ITK-KO
Percentage in CAR-T cells (%)
LAG-3
TIGIT
H
Raji only
Raji + nt-KO-CAR-T
Raji + ITK-KO-CAR-T
Days after CAR-T injection
-4
7
14
21
35
56
72
81
100
150
2.0 4.0 6.0 X10⁹
p/s/cm²/sr
I
Raji only
Raji + nt-KO-CAR-T
Raji + ITK-KO-CAR-T
Probability of Survival
Days after CAR-T injection
J
nt-KO
ITK-KO
Percentage in CAR-T cells (%)
CD45RO:
CCR7:
Naive
Effector memory
Terminally differentiated
Central memory
K
Ratio (Raji : CAR-T)
0h
24h
L
CAR-T cell number
PBMC only
PBMC + Raji
Fold change
0h
24h
M
PBMC only
PBMC + Raji
Percentage in CAR-T cells (%)
IFN-γ
TNF-α
Granzyme B

Figure 7

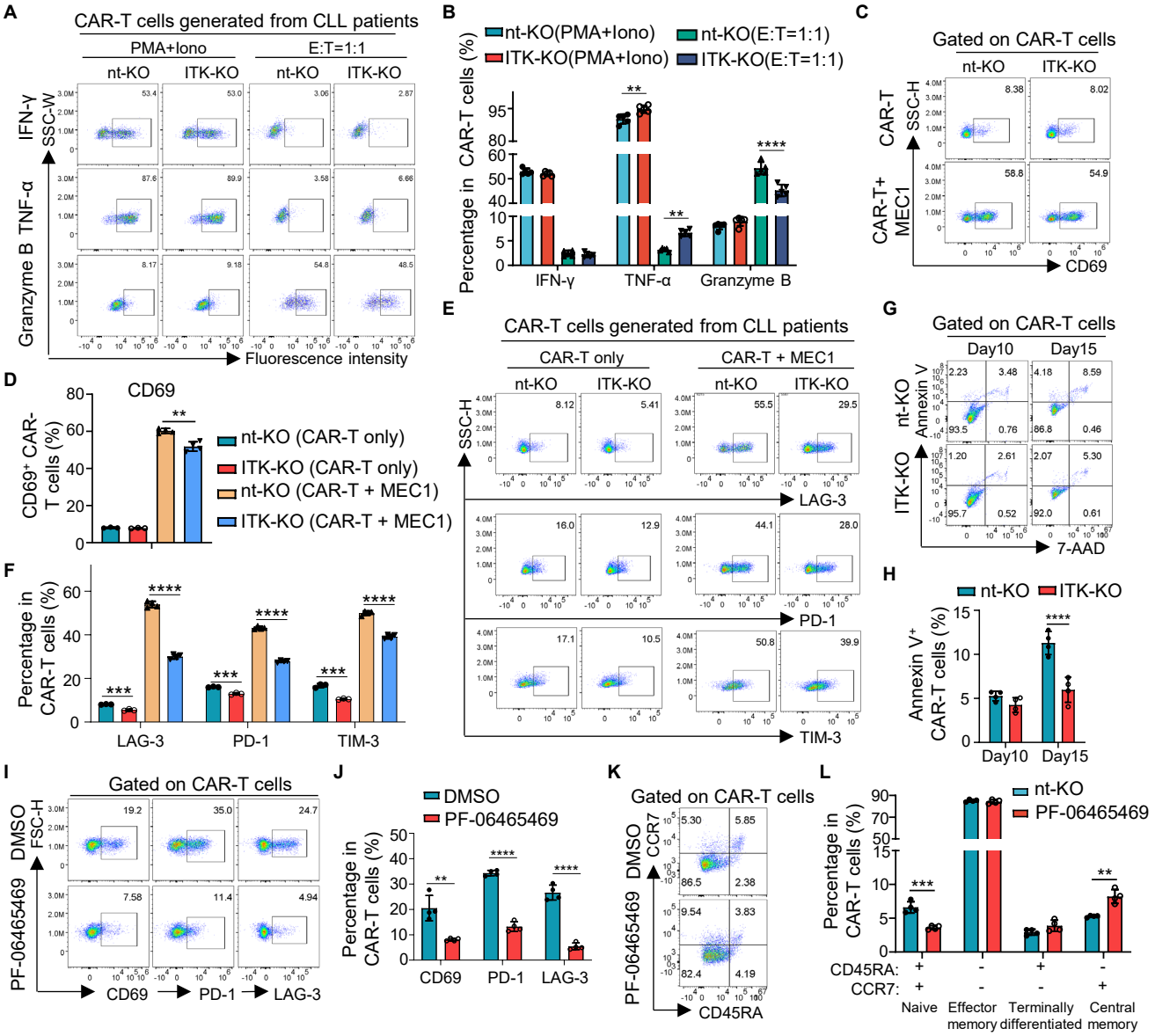
A
CAR-T cells generated from CLL patients
PMA+Iono
E:T=1:1
nt-KO
ITK-KO
IFN-γ SSC-W
Granzyme B TNF-α
Fluorescence intensity
B
nt-KO(PMA+Iono)
nt-KO(E:T=1:1)
ITK-KO(PMA+Iono)
ITK-KO(E:T=1:1)
Percentage in CAR-T cells (%)
IFN-γ
TNF-α
Granzyme B
C
Gated on CAR-T cells
CAR-T
CAR-T+ MEC1
SSC-H
CD69
D
CD69
CD69+ CAR-T cells (%)
nt-KO (CAR-T only)
ITK-KO (CAR-T only)
nt-KO (CAR-T + MEC1)
ITK-KO (CAR-T + MEC1)
E
CAR-T cells generated from CLL patients
CAR-T only
CAR-T + MEC1
SSC-H
LAG-3
PD-1
TIM-3
F
Percentage in CAR-T cells (%)
LAG-3
PD-1
TIM-3
G
Gated on CAR-T cells
Day10
Day15
nt-KO
ITK-KO
Annexin V
7-AAD
H
nt-KO
ITK-KO
Annexin V+ CAR-T cells (%)
Day10
Day15
I
Gated on CAR-T cells
DMSO
PF-06465469
FSC-H
CD69
PD-1
LAG-3
J
DMSO
PF-06465469
Percentage in CAR-T cells (%)
CD69
PD-1
LAG-3
K
Gated on CAR-T cells
DMSO
PF-06465469
CCR7
CD45RA
L
nt-KO
PF-06465469
Percentage in CAR-T cells (%)
CD45RA:
CCR7:
Naive
Effector memory
Terminally differentiated
Central memory

Figure 8

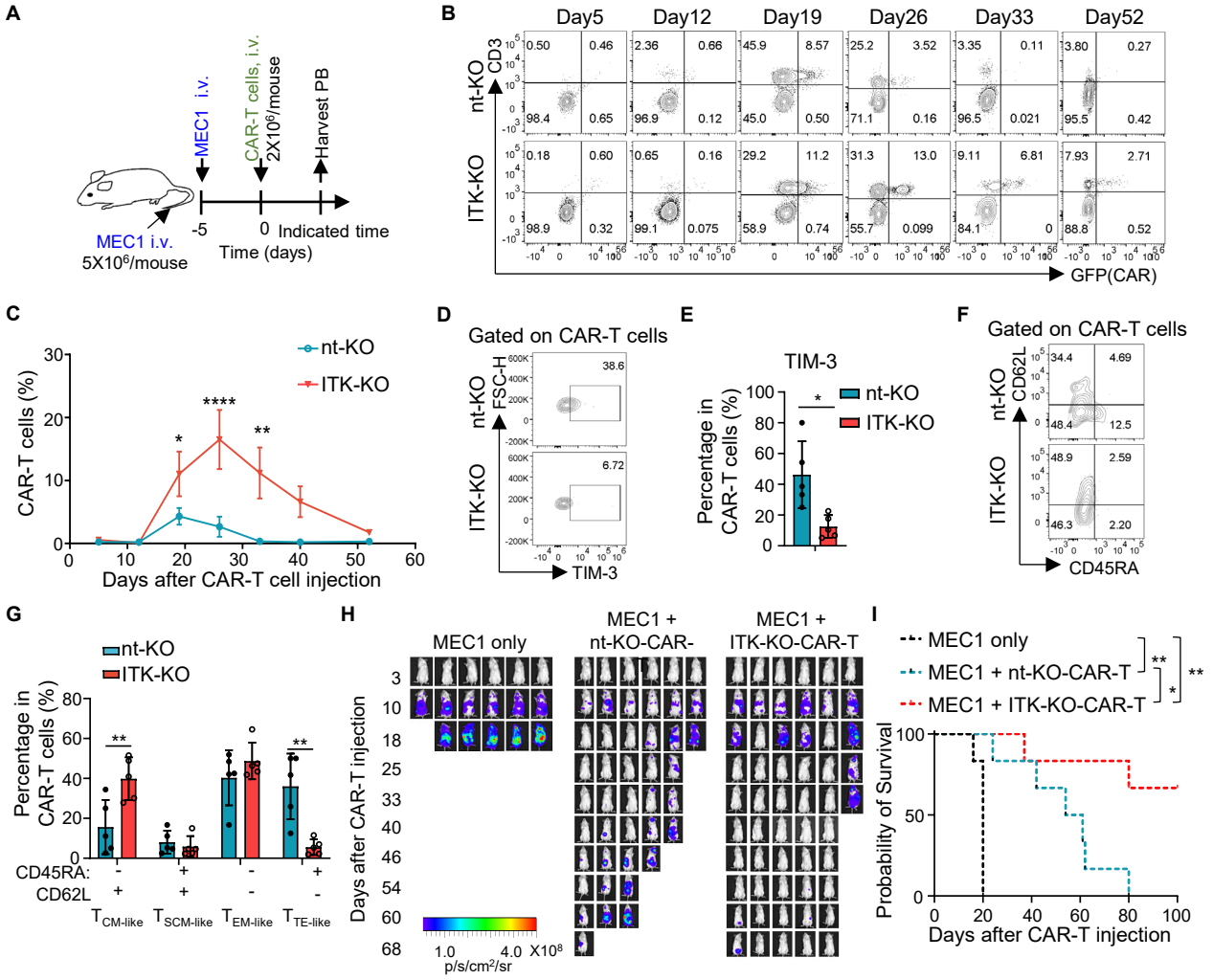
A
MEC1 i.v.
CAR-T cells, i.v.
2X10^6/mouse
Harvest PB
-5
0
Indicated time
Time (days)
MEC1 i.v.
5X10^6/mouse
B
Day5
Day12
Day19
Day26
Day33
Day52
nt-KO
ITK-KO
CD3
GFP(CAR)
C
nt-KO
ITK-KO
CAR-T cells (%)
Days after CAR-T cell injection
D
Gated on CAR-T cells
FSC-H
TIM-3
E
TIM-3
Percentage in CAR-T cells (%)
F
Gated on CAR-T cells
CD62L
CD45RA
G
Percentage in CAR-T cells (%)
CD45RA:
CD62L
T_CM-like
T_SCM-like
T_EM-like
T_TE-like
H
MEC1 only
MEC1 + nt-KO-CAR-
MEC1 + ITK-KO-CAR-T
Days after CAR-T injection
p/s/cm²/sr
I
MEC1 only
MEC1 + nt-KO-CAR-T
MEC1 + ITK-KO-CAR-T
Probability of Survival
Days after CAR-T injection